ABSTRACT

THOMPSON, TREVOR LEWIS. Investigation of Dielectric Spectroscopy as an Enabling Tool for Process Analytical Technology in 3D Biofabrication (Under the direction of Dr. Binil Starly).

Biofabrication is rapidly expanding usage and utility with applications towards drug screening, cell therapy and artificial tissue manufacturing being more viable. The processes for biofabrication consist of manufacturing living systems comprising cells and biomaterials used in both in vivo and in vitro applications. Effective and efficient quality assessment is a critical component to successful scale-up and expansion of biofabrication into industry practices. Current state of the art quality assessment is primarily applicable to 2D cell cultures and proves inefficient when translated to 3D distributions of the cells, resulting in delayed analysis and samples required for destructive testing. This work studies the use of dielectric spectroscopy (DS) as a method of process analytical technology (PAT) for 3D biofabrication, that fits within the quality by design (QbD) framework- an initiative developed by the Food and Drug Administration (FDA) for the pharmaceutical industry that incorporates real-time, non-destructive product monitoring into manufacturing processes. DS is used to assess the viable cell population, cell type and cell distribution through the correlation of dielectric parameters to critical to quality attributes (CQA) of biofabricated constructs. To evaluate the potential of DS to classify cells, studies were conducted over multiple days to monitor changes within cellular samples consisting of different cell types (liver and fibroblast cell lines). During the course of these studies, it was observed that permittivity readings- theorized to track number of viable cells- significantly changed over the course of 5 days ($p < 0.05$) for all types of cellular constructs; alamarBlue assay results also indicated a significant change in viable cell population ($p < 0.05$) over the 5 day studies.

Additionally, no significant changes occurred in critical frequency or α – both dielectric parameters that are theorized to be inherent to cell type- when compared within the same cell type ($p < 0.05$). Drug screening was also performed by administering different concentrations of acetaminophen (APAP) to cellular constructs containing liver cell lines, followed by monitoring of dielectric properties once the APAP metabolized. These studies found a significant change in permittivity readings, dropping as drug dosage is increased ($p < 0.05$). At the highest dosage of drug testing, the critical frequency increased significantly ($p < 0.0001$) indicating changes to cellular morphology. This investigation, of cellular constructs both over time and when exposed to drug screening, supports DS as an appropriate method of PAT in the field of biofabrication.

Investigation of Dielectric Spectroscopy as an Enabling Tool for Process Analytical Technology in 3D Biofabrication

by
Trevor Thompson

A thesis submitted to the Graduate Faculty of
North Carolina State University
in partial fulfillment of the
requirements for the degree of
Master of Science

Industrial Engineering

Raleigh, North Carolina

2019

APPROVED BY:

_____	_____
Dr. Binil Starly Committee Chair	Dr. Rohan Shirwaiker
_____	
Dr. Ashley Brown	

DEDICATION

To friends and family who have supported me and contributed positively in my life.

BIOGRAPHY

Trevor Thompson completed his B.S. in Industrial and Systems Engineering from North Carolina State University in May 2016. He joined the M.S in Industrial and Systems Engineering program at North Carolina State University in Fall 2016. He began working on his thesis at the 3D Tissue Manufacturing Lab under the guidance of Dr. Binil Starly in Fall 2016.

ACKNOWLEDGEMENTS

I would like to thank my thesis advisor, Dr. Binil Starly for his holistic vision that has not only contributed greatly to my research but has also always factored in my next steps beyond academia. His patience, wisdom and unique perspective are something I will strive to implement into my own life, even beyond professional or academic settings; it has been an honor having such a great mentor.

Thank you to the rest of my committee; Dr. Rohan Shirwaiker who has not only assisted in the understanding of my thesis, but also served as my professor for three courses total during my undergraduate and graduate degree. He has always been a phenomenal professor who helped originally spark my interest in biomanufacturing. I am grateful to Dr. Ashley Brown who has provided great input since I have taken her BME584 course; even being as kind as to answer my many questions after class.

Finally, I would like to thank colleagues that I have done research. In particular, Lokesh Narayanan has been a great mentor to give insight to my experiments, writing and studies. I am also grateful for Dr. Pedro Huebner, Parth Chansoria, and Karl Schuchard who have always been available to assist with experimental analysis and provide great office banter.

TABLE OF CONTENTS

LIST OF TABLES vii
LIST OF FIGURES viii
CHAPTER 1: INTRODUCTION 1
1.1. Biofabrication 1
1.2. Manufacturing Process Flow for Biofabrication 2
1.3. Problem Background 3
1.4. Research Objectives 4
1.5. Chapter Summary 6
CHAPTER 2: QUALITY 7
2.1. Quality by Design 7
2.2. Critical to Quality Attributes 9
2.3. Process Analytical Technology 10
2.3.1. Process Analytical Technology Tools 11
2.3.2. Risk-Based Approach 11
2.3.3. Integrated Systems Approach 12
2.3.4. Real Time Release 12
2.4. Chapter Summary 12
CHAPTER 3: DIELECTRIC SPECTROSCOPY 14
3.1. Critical to Quality Attributes of Cells 14
3.2. Theory of Dielectric Spectroscopy 15
3.2. Dielectric Spectroscopy for Cell Monitoring 16
3.3. Beta-Dispersion Spectra and Dielectric Properties 18
3.4. Former Applications 20
3.5. Chapter Summary 21
CHAPTER 4: MATERIALS AND METHODS 23
4.1 Cell Expansion 24
4.2. Alginate Preparation 25
4.3. Casting Process 25
4.4. Drug Dispensing 26
4.5. Assays 26
4.6. Dielectric Spectroscopy Assessment Methodology 27
4.7. alamarBlue Assay Curve 29

4.8. Data Analysis....29
CHAPTER 5: RESULTS AND DISCUSSION....31
5.1 Research Objective 1....31
5.2 Research Objective 2....36
5.3. Chapter Summary....41
CHAPTER 6: CONCLUSIONS....43
6.1. Conclusions and Contributions....43
6.2. Future Work....43
6.2.1. Inclusion of DS for On-Line Monitoring of Bioprints....43
6.2.2. Dielectric Probe Studies....44
6.2.3. More Complex Cellular Constructs for Drug Modeling....44
6.2.4. Imaging Cellular Constructs....44
REFERENCES....46
APPENDICES....53
Appendix A: Output of HepG2 (0g of APAP) Permittivity Readings....54
Appendix B: alamarBlue Assay Curve Readings....54
Appendix C: NIH/3T3 Dielectric Responses for Research Objective 1....55
Appendix D: HepG2 Dielectric Responses for Research Objective 1....55
Appendix E: Co-Culture Dielectric Responses for Research Objective 1....55
Appendix F: NIH/3T3 Dielectric Responses for Research Objective 2....56
Appendix G: HepG2 Dielectric Responses for Research Objective 2....56
Appendix H: Co-Culture Dielectric Responses for Research Objective 2....57

LIST OF TABLES

Table 1: Experimental design for Research Objective 1…….31
Table 2: Dielectric parameters of each cell type measured
for Research Objective 1 on Day 1 of the studied…...……..36
Table 3: Experimental design for Research Objective 2…….36

LIST OF FIGURES

Figure 1: Outline of traditional Quality by Testing (QbT) methodology……8
Figure 2: Outline of Quality by Design (QbD) methodology……...8
Figure 3: Differences between cells with an intact cell membrane and cells with a ruptured cell membrane when in the presence of an electric field……...…….17
Figure 4: Expected dielectric permittivity response as frequency increases ……..19
Figure 5: Overview of experimental studies……...24
Figure 6: Set up of ABER FUTURA probe and specifications……..28
Figure 7: β-dispersion for HepG2 on Day 3 compared to Day 5 with the dielectric parameters for HepG2 on Day 3 noted……..32
Figure 8: Top Left: Δε for NIH/3T3 cellular constructs and corresponding alamarBlue Reduction % across each day of dielectric monitoring. Top Right: An alamarBlue assay curve with line of best fit based off aB% for 1 million, 2 million and 5 million cells per NIH/3T3 cellular construct. Bottom: Corresponding Δε, aB% and estimates of cell count per sample based on alamarBlue assay curve……..……..33
Figure 9: Top Left: Δε for HepG2 cellular constructs and corresponding alamarBlue Reduction % across each day of dielectric monitoring. Top Right: An alamarBlue assay curve with line of best fit based off aB% for 1 million, 2 million and 5 million cells per HepG2 cellular construct. Bottom: Corresponding Δε, aB% and estimates of cell count per sample based on alamarBlue assay curve……..……..34
Figure 10: Top Left: Δε for Co-Culture cellular constructs and corresponding alamarBlue Reduction % across each day of dielectric monitoring. Top Right: An alamarBlue assay curve with line of best fit based off aB% for 1 million, 2 million and 5 million cells per Co-Culture cellular construct. Bottom: Corresponding Δε, aB% and estimates of cell count per sample based on alamarBlue assay curve……..……..35
Figure 11: Comparisons of Δε between cell types when exposed to different doses of acetaminophen and the *fc* value……..……..38
Figure 12: LIVE/DEAD images of biofabricated constructs consisting of (a) NIH/3T3 cells exposed to 0g APAP (b) HepG2 cells exposed to 0g APAP (c) Co-culture of NIH/3T3 and HepG2 cells exposed to 0g APAP (d) NIH/3T3 cells exposed to 4g APAP (e) HepG2 cells exposed to 4g APAP (f) Co-Culture of NIH/3T3 and HepG2 cells exposed to 4g APAP……...39
Figure 13: β-dispersion of HepG2 with 0g of APAP, HepG2

with 4g of APAP and Co-Culture with 4g of APAP……..40
Figure 14: Dielectric parameters of each cell type after exposure to specified dose of Acetaminophen during the study for Research Objective 2……...41

CHAPTER 1: INTRODUCTION

1.1. Biofabrication

The field of tissue engineering and regenerative medicine (TERM) has emerged to combat disease and organ failure that threaten the quality and duration of human life. Defined as "the application of principles and methods of engineering and life sciences toward fundamental understanding of structure-function relationships in normal and pathological mammalian tissues and the development of biological substitutes to restore, maintain, or improve tissue function" by the National Science Foundation, TERM focuses on the production of living biological systems that function as substitutes for systems that were previously only available in natural biological entities [1]. Three general strategies have been cultivated with the goal of recreating human tissue: isolated cells in the form of cell therapy, tissue-inducing substances in the form of growth factors and other external regulatory mechanisms that influence cell growth, and cells placed in 3D environments to replicate the structure of tissue [2]. While cell therapy and substance delivery have shown benefit in the past, current technological trends have prioritized new focus in new research to enable tissue engineering in the form of 3D fabrications.

Biofabrication is a facet of TERM that can be defined broadly as the conjunction of biological materials into fabricated constructs [3]. The combination of biological and biologically compatible materials is done additively with the most popular technique being bioprinting in which cellular material is extruded to form unique geometries in accordance to 3D positioning [4]. Biofabrication has applications in artificial tissue manufacturing, disease modeling and the studying of cells and bioactive components due to a customizable 3D

organization that can best mimic in vitro conditions [5]. These current applications aim to solve issues associated with deteriorating health such as organ failure.

Other potential solutions to the diseases that cause organ failure, is in the form of pharmaceuticals that undergo extensive and costly regulatory validation before reaching human trials with only 10% of products making it through clinical development [6]. Validation often includes animal drug screening which is not always an accurate assessment of clinical efficacy of pharmaceuticals for certain human tissue types [7,8]. Due to the concerns of ethicality, feasibility, accuracy and cost of animal trials alternatives are being sought to conduct drug screening. Recently, biofabricated tissue models are being applied to drug screening in what is the most imminent use of the technology due to the lower level of complexity associated with manufacturing a small scale organ to serve for toxicity testing compared to an entire artificial tissue for transplant [9]. Manufacturing the necessary components for these complex biological products is vital for the success of biofabrication, regardless of the application.

1.2. Manufacturing Process Flow for Biofabrication

The manufacturing process for biofabricated constructs begins with harvesting cells [10–13]. Cell harvest can be classified as either autologous (sourced from the person who is the intended patient for the application), allogenic (sourced from an acceptable match to the intended patient of the application) or xenogeneic (sourced from a different species than the intended patient of the application) [14]. For the most accurate results cells harvested for biofabrication should be autologous [15,16]. Once cells are harvested, cells are expanded to reach the appropriate population needed for the application of biofabrication. Then, through the use of additive manufacturing techniques, cells can be combined with biomaterials and dispensed layer by

layer, stacked on top of one another to form engineered tissues and organs [17]. Harvesting cells, culturing cells to the appropriate number and then utilizing cells in 3D biofabricated constructs are a multi-step process with several interactive parameters that comprise the manufacturing process.

1.3. Problem Background

During the processing flow for manufacturing biofabricated products, several concerns arise affecting the overall functionality and efficacy of the final product. For biofabrication to be considered functional the cells composing the end result must be the intended cell type, with specified spatial distribution and high viability [5,18]. As with any manufacturing process, the processing parameters utilized to generate the product can have adverse effects on the quality of the materials used to manufacture- in this case, cells [19]. When in the presence of environmental stimuli, cells can react with a myriad of changes impacting product quality. These changes include alterations to cellular morphology- which dictates how cells interact with one another-, cellular migration – a prominent component of tissue repair, immune surveillance and cell functionality -, differentiation- cells changing into other cell types through the use of transcription factors - or metabolic rate- the construction of key enzymes for essential cellular function and breaking down of molecules for energy [20,21]. Additionally, certain processing parameters can cause cells to undergo necrosis- cell death through environmental stimuli- resulting in fewer viable cells within a sample [22]. As with the most successful manufactured items, continuous and accurate quality assessment is critical to reduce cost associated with scrap and to ensure that the end result functions as intended. Although quality assessment measures are available for biofabricated constructs, current methods are lacking functionality which creates a challenge for scale-up.

The most common practice of cellular quality assessment consists of histological and biochemical assays. These assays are used to evaluate viability and metabolic rate (in the case of LIVE/DEAD®, alamarBlue® L-Lactate®, MTT®), permeability (in the case of CultureCoat®, Caco-2) and cell differentiation (in the case of Alizarin red staining); however, these assays cannot be done in real time and have yielded mixed results when applied to 3D culture [23–25]. Additionally, these assays are often destructive- requiring a sample to be used solely for testing- and during the testing can even have results mixed due to stress dealt to the cells during the assay process [26].

When applied to drug screening, the need for an identical sample testing and the lack of real time results is problematic. Typically, drug screening responses are tracked over time to determine the interactions the drug has with the body as it is metabolized [27]. In cases of tracking cellular viability, in vitro models utilizes trypan blue and other assays to predict the concentration of live cells [28]. Although this determines the percentage of viable cells, it sheds no knowledge on the number of viable cells in a sample which is a critical factor for predicting drug metabolization and lethal drug dosage [29]. These assays are also not suitable for 3D biofabricated constructs. Due to these concerns, as biofabrication begins to scale up from a research setting to an industrial production system, new quality control methods must be explored to assure real-time and accurate monitoring of cellular components. Given that drug screening is the most imminent and likely application of biofabrication subject to scale up, new quality control methods must also be able to detect changes caused by interactions with drugs.

1.4. Research Objectives

In this work, two key research objectives are investigated to contribute to the state of quality monitoring in the field of tissue engineering:

Objective 1: Determine the β-dispersion Characteristics of 3D Biofabricated Constructs (Comprising NIH/3T3, HepG2 and a Co-Culture of NIH/3T3 & HepG2) Over the Course of 5 Days

Create a reference table for three types of cellular constructs- NIH/3T3 (Mus musculus embryo fibroblast cells), HepG2 (Homo sapiens hepatocellular carcinoma cells) and a co-culture of HepG2 and NIH/3T3 - detailing the dielectric properties of each cellular construct at a given concentration of 5 million 100% viable cells encapsulated in 1mL of crosslinked 2% (w/v) alginate hydrogel.

Objective 2: Investigate the Response of β-dispersion Characteristics When Exposed to Acetaminophen

Monitor the dielectric properties of three types of cellular constructs- NIH/3T3, HepG2 and a co-culture of HepG2 and NIH/3T3- after a 24hr exposure to acetaminophen at 3 doses- 1g, 2g and 4g. Each cellular construct will be at a given concentration of 5million cells and encapsulated in 1mL of crosslinked 2% (w/v) alginate hydrogel.

The contributions of this thesis include:

- Assessment of a nondestructive method to evaluate the quality of biofabricated constructs in real-time.
- Detailed quality evaluation of the dielectric properties of specific cell types which can be used to evaluate critical quality attributes of future biofabricated constructs.
- Investigate the relationship between changes in dielectric properties of cells in response to controlled drug exposure

1.5. Chapter Summary

Biofabrication has the potential for use in cell therapy, drug screening and artificial tissue manufacturing. As the uses of biofabrication become more common in industry, quality assessment will be a critical component of success to ensure the process control and intended functionality of products. Currently methods of quality assessment that are applied to biofabrication lack functionality as assays were developed for 2D cell culture and require offline testing that is oftentimes destructive to cells. The limitations of previous approaches to get real-time, continuous results have created a need to establish new quality monitoring techniques that are applicable to biofabrication to ensure the advancement of manufacturing biological systems. Put forth by two objectives, this study will assess the efficacy of a new quality monitoring method in the case of multiday studies of cellular constructs and drug screening studies of cellular constructs.

CHAPTER 2: QUALITY

2.1. Quality by Design

Current quality assessment methods can be best described as quality by test, consisting of batch testing at set checkpoints during the manufacturing process. These checkpoints comprise raw material testing and end product testing all of which requires fixed product manufacturing processes in order to mitigate quality risks between raw material acceptance and end product results [30]. When using current quality control practices several disadvantages occur; products that are out of quality specification are often times discarded resulting in high scrap rate and associated cost, root causes of product failure are typically not well understood resulting in a manufacturing process with a likelihood to spoil further batches, additionally changes to the manufacturing processes require the manufacturer to file supplements with the FDA constraining manufacturers to processes that were originally approved until a lengthy approval is completed [31]. Although quality by test methods have been used across industries for several decades, new quality assurance methods have been proposed to improve efficiency and efficacy [32].

Quality by Design (QbD) is an initiative put forth by the FDA under its guidelines for current Good Manufacturing Practices (cGMP) that details methods of integrating quality into the design of manufacturing processes rather than testing quality after manufacturing processes have occurred. The success of QbD is contingent on the idea of a dynamic control strategy that combines quality monitoring with adaptive set points and operating ranges that can be adjusted once feedback occurs in conjunction with in-process monitoring [33]. The first step to implementing quality by design into a manufacturing process consists of setting a Quality Target Product Profile (Q-TPP) which is a summary of quality characteristics to be achieved

once manufactured. To accurately define the desired quality target product profile the necessary properties to be monitored during manufacturing must be defined as well [30]. These properties are split into three categories: Critical to Quality Attributes (CQA), Critical Material Attributes (CMA) and Critical Process Parameters (CPP). Critical Material Attributes refers to the physical, chemical or biological properties of an input material; these are to be monitored prior to integration into the manufacturing process to ensure the desired quality and quantity of in-process material. Critical Process Parameters are the manufacturing parameters that are to be monitored in process due to the influence it has on the purity, yield and function of the final product. Critical to Quality Attributes are quantifiable attributes of a product to be monitored in-process or after-process due to the potential impact on safety and efficacy. CQA, CMA and CPP are multivariate factors integral in determining the end quality target product profile. Typically, CPP are known inputs into manufacturing processes while CMA can be assessed prior to processing; therefore, more emphasis will be placed on CQA.

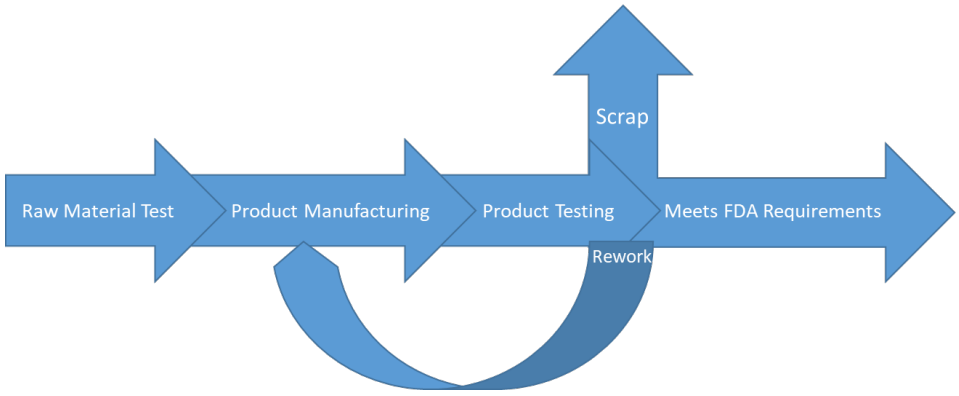

Figure 1: Outline of traditional Quality by Testing (QbT) methodology

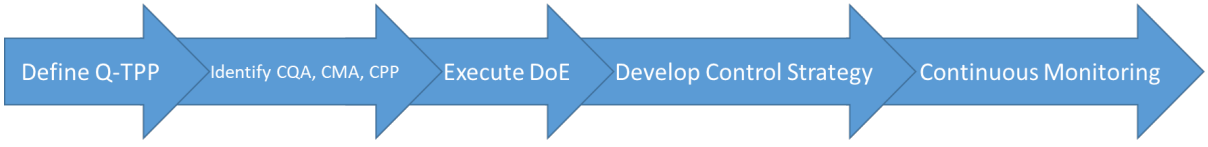

Figure 2: Outline of Quality by Design (QbD) methodology

2.2. Critical to Quality Attributes

The International Council for Harmonisation of Technical Requirements for Pharmaceuticals for Human Use (ICH)- a collaborative organization that corresponds with both the pharmaceutical industry and regulatory bodies- defines CQA as "A CQA is a physical, chemical, biological, or microbiological property or characteristic that should be within an appropriate limit, range, or distribution to ensure the desired product quality." [34]. Though initially applied to the pharmaceutical industry, the term is prevalent across all forms of biotechnology [35–37]. When used as a pillar of QbD, CQA must be well defined and well monitored throughout the manufacturing process. Defining CQA is product specific and should have a direct link to desired output defined by the Q-TPP. Establishing what CQA is, requires appropriate testing and correspondence of potential CQAs to well defined Q-TPP of end products [33]. This testing should give a direct relationship to a CQA and the targeted function of the final product [31].

CQA can be thought of as a response variable of the CPP that indicates the effect of the process parameters has on overall product quality. Therefore, effective and efficient monitoring of CQA in the form of accurate and timely product analysis is a critical component of process control. Accurate monitoring of CQA can be performed in a few ways:

- off-line: monitoring consists of samples of products being taken away from the manufacturing process stream- typically at the end of the process stream- and being assessed for CQA to be within specification.
- at-line: monitoring is conducted where the sample is removed from the manufacturing process stream and then assessed for CQA to be within specification.
- on-line: monitoring takes place as a sample is diverted from the manufacturing process stream, only to be returned once CQA assessment has occurred.

- in-line: monitoring takes place within the manufacturing process stream with no removal or diversion necessary to gather data for CQA assessment.[38]

Traditionally, off-line and at-line quality monitoring has occurred in the form of quality assurance checks once the product has been manufactured or a verification protocol that occurs during manufacturing. Though helpful in the past and still prevalent in some industries today, the results gathered from these tests are met with a lag time that can cause significant scrap rate and increased cost that is not suitable for the biotechnology sector where manufacturing costs are already high [39,40]. QbD aims to alleviate this hefty cost by assessing CQA during the manufacturing process in the form of on-line or in-line monitoring [41].

When in-line or on-line monitoring methods are incorporated into the manufacturing process, real-time feedback occurs. Real-time feedback describes an assessment that is made in process to efficiently provide analysis of a product. This can be integrated into a feedback control loop that adjusts critical process parameters to optimal values to compensate for CQA when out of specification [42]. The result is a robust system that can correct for variables affecting the manufacturing processes that negatively impact the CQA profile of an in-process product. Once the CQA profile of a final product is verified to be within the acceptable quality limits dictated by the Q-TPP, based on real-time measurements, then produced goods can be safely released on the basis of quality monitoring data alone and require no further quality assurance [43]. To achieve these real time measurements appropriate sensing technology must be applied to the analysis of the manufacturing process.

2.3. Process Analytical Technology

The term Process Analytical Technology (PAT) has been used to describe measurement technologies and physical characterization tools in the field of process analytics for well over a century, with the terms use dating back to 1911 [44]. However, as the manufacturing

industry has evolved, PAT is becoming a common term to control and analyze manufacturing processes. Although this technology applies ubiquitously, across industries, the FDA has recently come to define the term as such:

"a system for designing, analyzing, and controlling manufacturing through timely measurements (i.e., during processing) of critical quality and performance attributes of raw and in-process materials and processes, with the goal of ensuring final product quality." [38]

Expounding on this the FDA wrote a guidance describing the framework of PAT that outlines the risk-mitigating framework in which industries can advance process understanding, improve data collection and innovate quality control practices specifically in pharmaceuticals, but more broadly, in any industry the organization oversees.

While the implementation of PAT varies, pending on the application, the general framework for appropriate use of this system finds basis in four main principles:

2.3.1. Process Analytical Technology Tools

To mitigate risk appropriate data must be taken during manufacturing process. Data must be taken through multivariate sources for assurance of root cause [43]. This data is collected through a process measurement system that monitors all critical to quality attributes. Feedback loops should be in place so that process controls can provide adjustments to account for all critical to quality attributes and modify processes when these attributes are out of specification.

2.3.2. Risk-Based Approach

When implemented PAT is reliant on a risk-based approach that has an inverse relationship between process understanding and the risk of inadequate product quality. PAT is dependent

on the practice of continuous learning through data collection and analysis. Information technology infrastructure that forms from this data must be managed by a knowledge of regulatory decision making.

2.3.3. Integrated Systems Approach

PAT integrates the functions of development, manufacturing, quality assurance and information/knowledge management into a concurrent product process.

2.3.4. Real Time Release

Real time release is founded on the principle that process data is indicative of the final product quality as the product moves through the manufacturing process stream. Process data is collected through direct and indirect process analytical methods that utilize PAT tools that monitor continuously throughout manufacture. By using the process data collected throughout manufacture, in lieu of final product quality assessment, standards for product testing and release for distribution-21 CFR 211.165- are fulfilled while reducing lead time and storage inefficiencies.

The development and implementation of PAT is consistent with the tenants of QbD and is compatible in the goal of improving efficiency through reducing quality concerns. PAT is a critical component in establishing accurate and efficient feedback to processing parameters as well as identifying in-process products that could be out of Q-TPP specification and subject to rework to salvage the product instead of the product becoming scrap upon final inspection.

2.4. Chapter Summary

Originally implemented by the FDA for the pharmaceutical industry, quality by design is a framework that incorporates quality assurance into the manufacturing system design through

the use of process analytical technology to measure critical to quality attributes, monitor the variability of the process through these quantifiable attributes and adjust process parameters through a feedback loop. Proper application of quality by design through the use of established relationships between measured attributes and final product function results in a robust system where quality is a part of the manufacturing process and requires no additional product testing. This framework is also finding use in the biotechnology industry where production costs are high and products are complex, heterogeneous systems. Identification of CQA of biofabricated products and the appropriate process analytical technology can deliver real-time feedback that ensures product quality and facilitates necessary process parameter adjustment consistent with the QbD framework.

CHAPTER 3: DIELECTRIC SPECTROSCOPY

3.1. Critical to Quality Attributes of Cells

Successful manufacturing of biofabricated products is a nuanced and multifaceted set of specifications that requires proper cell type, cellular alignment, cell population and cell viability. Cell type has a myriad of effects on overall tissue function including structural function, vascularization, maintaining other cells [45]. Cell type can also provide a niche for stem cell maintenance and differentiation, a necessary function when in vivo where stem cells are present [46]. Cell type can change, if differentiation occurs, making keeping track of the cell type an essential component to successfully manufacturing biofabricated constructs. Cellular alignment is critical to facilitating proper alignment of the extracellular matrix (ECM) of a biofabricated construct. ECM is a collection of macromolecules secreted from cell- the type of secretion is dependent on the type of cell [47]. The ECM provides the structural integrity for tissue; therefore, ECM is a determining factor of the quality of a biofabricated construct. As advances are made in biofabrication, the proper spatial distribution of cells will become more critical in order to ensure that vascularization of tissue can occur [48].

The appropriate number of cells within a sample can determine the success of a biofabricated construct. While the exact number of cells needed for proper tissue function depends on the type of tissue, too few cells risk tissue failure due to the low overall rate of cellular proliferation and low rate of ECM secretion [49]. Too few cells can also change the trajectory of differentiation resulting in an unwanted cell type if not at adequate cell density [50]. While too many cells can result in inadequate nutrition and oxygen transport resulting in cell death [51].

Cells viability is the ratio of live cells to dead cells; live cells are intact and capable of proper protein expression while dead cells are unable to proliferate or produce proteins [52]. Protein expression is a defining component of cellular function and needs to be achieved as expected in order for a biofabricated construct to function as expected. In addition to needing a proper number of viable cells to achieve the desired functionality of a biofabricated construct, it has been shown that non-viable cells have inhibitory effects on the viable cell population hindering antibody production [53]. A critical characteristic of viable cells is an intact membrane- protecting the organelles responsible for protein production that determines the functionality of the cell [54].

The target quality product profile, regardless of application, requires appropriate CQA to be in specifications. In biofabrication, the aforementioned specifications serve as CQA: cell type, cell distribution, cell number and cell viability. Identification of CQAs of biofabricated constructs leads to the next need in implementing the QbD framework: selecting appropriate monitoring equipment to serve as PAT and pairing the measurements taken from monitoring to establish a relationship to CQA.

3.2. Theory of Dielectric Spectroscopy

Dielectric Spectroscopy (DS) is the method of measuring intrinsic electrical properties of a dielectric material. A dielectric material is any system that is an electrical insulator whereby the flow of electrons is impeded by insulating properties of the material; unable to flow freely through the material electrons shift only slightly away from equilibrium positions within the dielectric material [55]. When electron movement is facilitated by an electric field, the material becomes polarized reducing the overall force of the electric field within the

material. As frequencies of exposure vary, electrons within the material polarize at different rates resulting in different permittivity and conductivity values.

In the case of high-frequency response the dielectric constant (ε)- which is a ratio of permittivity of the dielectric to the permittivity of a vacuum- can be fit to the Cole-Cole model using the following equation [56,57]:

$$\varepsilon^*(\omega) = \varepsilon' - j\varepsilon'' = \varepsilon_\infty + \frac{\varepsilon_s + \varepsilon_\infty}{1 + (j\omega\tau)^{1-\alpha}} - \frac{j\sigma}{\omega\varepsilon_0}$$

Equation 1: Calculation of permittivity at a given frequency where $\varepsilon^*(\omega)$ is the relative complex permittivity as a function of frequency, $\varepsilon'$is the real part of the relative permittivity, ε'' is the imaginary part of the relative permittivity containing both conductivity and dielectric loss, ε_s is the static relative permittivity, ε_∞ is the optical relative permittivity, ε_0 is the permittivity of vacuum, 8.85 x 10^{-12} F m^{-1}, ω is the angular frequency (rad s^{-1}), τ is the relaxation time (s), σ is the conductivity of the fluid (S m^{-1}) and α is the distribution factor

When the Cole-Cole model is applied to a dielectric substance the Maxwell-Wagner effect is observed in which as frequencies increase interfacial polarization occurs resulting in capacitor effects impacting the permittivity of samples [58]. Given that the imaginary portion of the calculation for permittivity is based on the resting potential of the sample being measured, each dielectric measured interacts differently across a spectrum of frequencies which can be used to classify the composition of the sample without contact [59–61]. Given that DS is non-destructive and can provide real-time results indicating the properties of any dielectric substance, it has the potential to be applied to biological systems.

3.2. Dielectric Spectroscopy for Cell Monitoring

Viable cells maintain a semi-permeable membrane that provides structure to the cell and maintains the intracellular cytoplasm and organelles. The cellular membrane consists of a non-conductive phospholipid bilayer acts as a double shell structure separating conductive media and enclosed cytoplasm that is also conductive. Due to this insulating separation, the membrane provides the ions within the cell and outside of the cell makes living cells behave

as electrical capacitors when exposed to electric fields [62]. In cellular media and intracellular space, ions are free floating and displace in response to the electric field only to accumulate at cellular membranes. In healthy cells with intact membranes, the cell membrane circumscribes cytoplasmic ions leading to a buildup of opposing charges both sides of the thin phospholipid bilayer membrane. Intact cell membrane provides a separation between the accumulated positive and negative charge causing the cell to behave like a capacitor. Alternatively, dead or dying cells will hold no charge along the cellular membrane due to the rupture of the damaged cell membrane caused by apoptosis or necrosis [22].

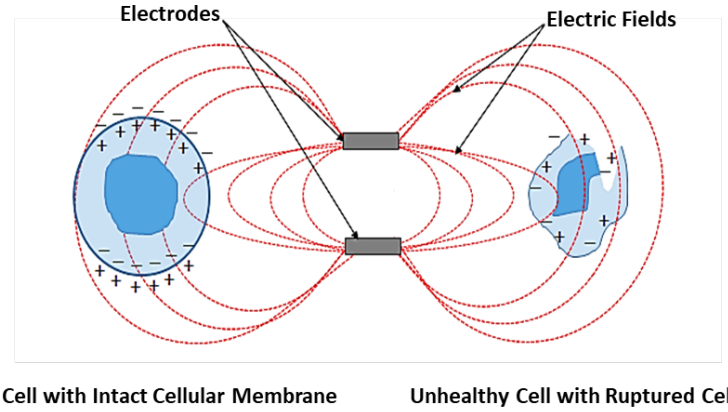

Figure 3: Differences between cells with an intact cell membrane and cells with a ruptured cell membrane when in the presence of an electric field

Knowledge of these differences contribute significantly to drug screening where the morphology of cells changes notably when exposed to drugs. When metabolizing drugs, cells undergo either apoptosis or necrosis. Necrosis is the rupturing of a membrane through cell swelling and is theorized to change dielectric parameters in ways that correspond to viable cell population and distribution. Apoptosis creates a unique circumstance in which membrane properties are changes and cells shrink which can theoretically change dielectric parameters associated with cell type and viable cell population. The proportion of apoptosis vs necrosis as a product of drug toxicity has been the subject of debate with some studies indicating a

high rate of apoptosis in rat studies while other groups detected oncotic necrosis [63,64]. Intracellular signaling and regulatory mechanisms support the concept that there exists a close relationship between apoptosis and necrosis supporting the notion the dielectric parameters may detect distinct differences in permittivity readings [65]. This distinction between intact membranes and damaged membranes is indicated by differences in permittivity readings across a range of frequencies that correspond to dielectric parameters that can be monitored within cell samples using DS.

3.3. Beta-Dispersion Spectra and Dielectric Properties

The spectra of permittivity values across a frequency range results in a graph consisting of an inverted sigmoid shape. When graphed, as in Figure 4, the spectrum of frequencies results in 3 distinct regions can be distinguished due to changes in the slope: the α-dispersion, the β-dispersion and the γ-dispersion. The α-dispersion occurs at low frequencies. The low frequency range allows intracellular and extracellular ions to have adequate time to accumulate across the cell membrane resulting in higher interfacial polarization [66]. In the low frequencies of the α-dispersion, there is a measure of resting potential of the cells in a sample, but this lacks appropriate dielectric sensitivity necessary for quality monitoring [67]. At the other end of the spectrum, γ-dispersion occurs at high frequencies where ions do not have enough time to polarize at the cellular membrane, resulting in low permittivity readings [68]. This γ-dispersion is indicative of the permittivity of the media environment but is not suitable for quality monitoring cellular samples [69]. Between the α-dispersion where the cell membrane is highly polarized and γ-dispersion where it is not, there is a steady decrease in permittivity as frequency increases. This results in a region of interest referred to as the β-dispersion.

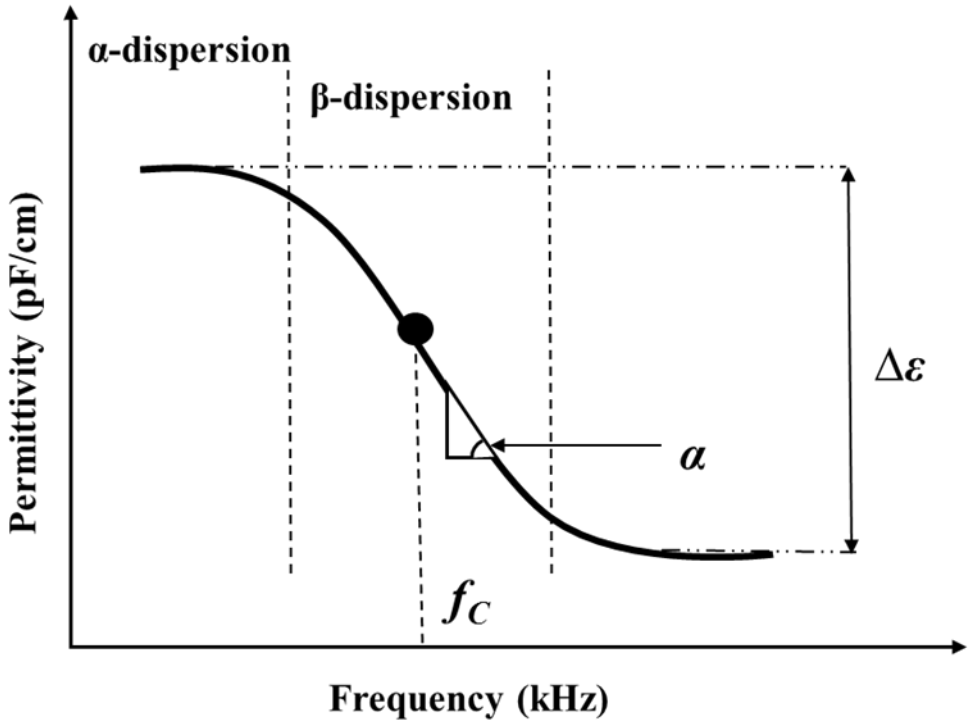

Figure 4: Expected dielectric permittivity response as frequency increases

The β-dispersion is characterized by three important parameters – delta permittivity *(*$\Delta\varepsilon$), critical frequency (f_c) and cole-cole alpha (α). The difference between the permittivity in the high permittivity-low frequency region and low permittivity-high frequency region of the β-dispersion is referred to as the $\Delta\varepsilon$. The $\Delta\varepsilon$ is proportional to the total volume of viable cells as well as the mean radius of the cells present in the measurement volume as shown in Equation 2 [70].

$$\Delta\varepsilon = \frac{9 \cdot P \cdot r \cdot C_m}{4\varepsilon_0}$$

Equation 2: Calculation for Δε where P is the volumetric fraction of viable cells (i.e., volume of material bounded by the cell membrane per unit measurement volume), r is the radius of nominally spherical cells, C_m is the cell membrane capacitance per unit area, and ε_0 is the permittivity of free space (8.854 x 10-12 F/m).

Delta permittivity values can be monitored regularly through frequency scans of a dielectric spectroscopy probe. This provides real-time feedback of values that correspond to viable cell population.

The frequency corresponding to the midpoint of the β-dispersion slope is referred to as the critical frequency (f_c) [71,72]. The f_c is is inversely proportional to the mean cell radius and intrinsic properties of the cell such as membrane conductivity. Due to these intrinsic cellular properties corresponding to f_c values, this dielectric parameter is expected to distinguish given cell type regardless of the total viable cell volume as shown in Equation 3 [73–75].

$$f_C = \frac{1}{2\pi \cdot r \cdot C_m(\frac{1}{\sigma_i'} + \frac{1}{2\sigma_0'})}$$

Equation 3: Calculation for f_c Where σ_i' is the internal cytoplasmic conductivity of the cells within the measured sample and σ_0' is extracellular conductivity, r is the radius of nominally spherical cells, C_m is the cell membrane capacitance per unit area. C_m, r, σ_i', and σ_0' are intrinsic constants for a given cell type.

The slope of the β-dispersion is referred to as the Cole-Cole α. The dimensionless α corresponds to τ (relaxation time) and the number of dipoles formed during the interfacial polarization across the cell membrane [76,77]. The value for α has been shown to be related to cell size distribution within the measured volume [71,78]. Through the correspondence of the three characteristic dielectric parameters to CQA of cells- delta permittivity *(*$\Delta\varepsilon$) paired to viable cell population, critical frequency (f_c) paired to cell type and Cole-Cole alpha (α) paired to cell distribution- DS demonstrates the potential to be used as PAT for biofabrication and other tissue engineering applications.

3.4. Former Applications

The potential for DS to be used as a diagnostic and quality assessment tool has been established in 2D cultures to assess biomass without damaging the cell samples [79–81]. In

3D environments, DS has been applied to fermenters to monitor bacterial and yeast activity while in suspension [74,82]. DS has also been applied to bioreactors, which provide a 3D non-adherent environment for proliferation of select cell lines, but also prevents an accumulation of ECM that is needed for in vivo comparison [83]. More recent developments of DS have included the detecting of cell morphology changes caused by temperature changes and the ability to distinguish healthy tissue from cancerous tissue [71,84].

In addition to DS other methods of quality assessment have been applied to biofabrication. Both near infrared (NIR) and mid-infrared (MIR) spectroscopy have been applied extensively to monitoring biofabricated constructs [30,39,85,86]. This method of detection provides fast, real-time results, but yields itself to inaccuracies in analysis due to overlapping of spectrum values [87]. Raman spectroscopy has been applied to 3D cultures to quantify viable cell population by measuring the amount of scattered light through the use of fiber-optics [88]. However, despite the use of DS and other analytical monitoring methods in both 2D and 3D cultures there still exists no study utilizing a non-destructive quality assessment tool capable of real-time feedback to indicating the changes cellular properties when exposed to drug screening.

3.5. Chapter Summary

Dielectric spectroscopy is a method of detecting the properties of any dielectric material. This technology operates by emitting and electric field and detecting corresponding changes to the flow of ions within the material. Given that cells used in biofabrication applications can act as a capacitor due to the insulating phospholipid bilayer separating intracellular and extracellular ions dielectric spectroscopy can used to determine properties that correspond to the CQA of biofabricated constructs: viable cell population, cell distribution and cell type.

When detecting dielectric properties of cells relative permittivity is measured across a spectrum of frequencies in which an indicative region known as the β-dispersion exists. The β-dispersion denotes three characteristic parameters delta permittivity (Δε), critical frequency (f_c) and cole-cole alpha (α) that correspond to viable cell population, cell type and cell distribution respectively. DS has been shown to distinguish cell type and populations within 2D environments demonstrating the potential for this technology to be used for real-time, non-destructive quality assessment of biofabricated constructs in multiple applications. Due to the utility of biofabricated constructs in drug screening applications, DS was selected to monitor changes in cells when exposed to acetaminophen.

CHAPTER 4: MATERIALS AND METHODS

To monitor the dielectric properties of biofabricated cellular constructs both over time and under drug exposure conditions two sets of experimental studies were conducted and outlined in Figure 5. The first set of studies consist of monitoring dielectric properties of cells when cast in 3D alginate constructs and made to sustain a lifespan of 5 days in in-vitro conditions. The dielectric parameters taken from this study were then compared with assay results in order to assess the corresponding number of cells in each sample. The second set of studies consisted of exposing cast cellular constructs to varying doses acetaminophen and subsequently monitoring changes in the dielectric parameters after the cellular constructs metabolized the acetaminophen. The dielectric properties taken from this study were then compared with the properties taken from healthy cell studies.

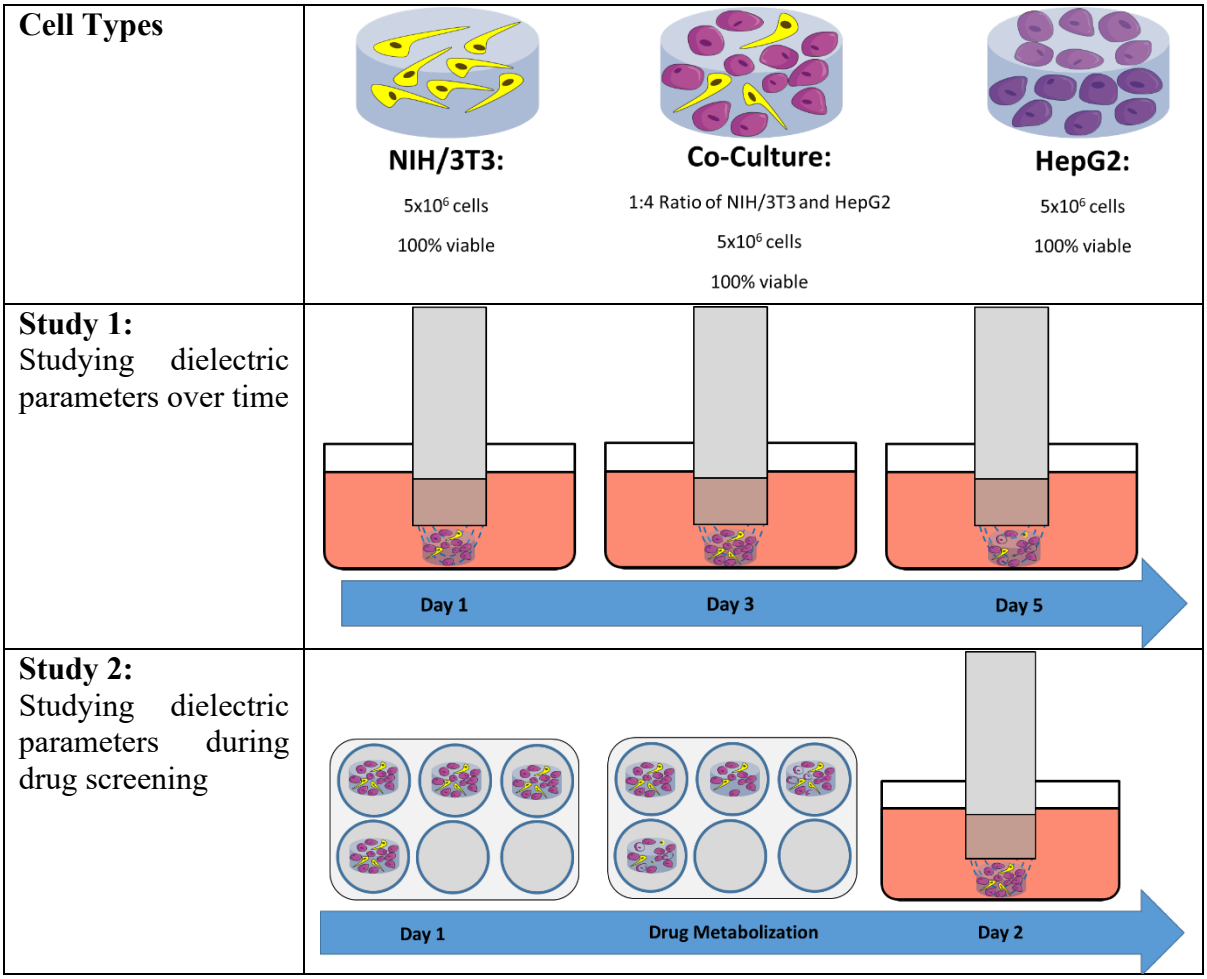

Figure 5: Overview of experimental studies

4.1 Cell Expansion

NIH/3T3 (ATCC® CRL-1658), HepG2 (ATCC® HB-8065) were all separately cultured in 15mL of prepared media, consisting of Minimum Essential Medium (MEM; Gibco, Grand Island, NY) supplemented with 10% heat-inactivated fetal bovine serum (FBS; Gibco) and 1% Antibiotic-Antimycotic (Gibco), in 75cm^2 cell culture flasks that were maintained at 37°C and 5% CO2. Each cell type was passaged when confluency was approximately 80%. Cells were harvested using 3mL of 0.25% trypsin EDTA (Gibco) subsequent to one wash

using 5mL of sterilized phosphate buffered saline (PBS). A hemocytometer was used to count the number of cells during cell passaging and for the preparation of the cellular constructs. Trypsinized cell solutions were neutralized with media. Cells were passaged at a seeding density of 250,000 cells/75cm^2 cell culture flasks.

4.2. Alginate Preparation

2% w/v alginate was prepared by mixing 0.6g of alcohol sterilized sodium alginate powder (WillPowder, Miami Beach, FL) with 29.4mL of sterilized phosphate buffered saline (PBS) in an ultrasonic water bath at 60Hz for 2 hours, based on an established protocol [89]. 2% w/v calcium chloride was prepared by mixing 10g of calcium chloride dehydrate (Signma-Aldrich; St. Louis, MO) with 490mL sterile deionized water.

4.3. Casting Process

All casted cellular constructs were made using 5 million cells total based on previously established cellular concentrations that were distinguishable using the same dielectric spectroscopy probe [90]. Single cell type constructs consisted of solely 3T3/NIH or HepG2 cells while the co-culture constructs consisted of 4 million HepG2 and 1 million 3T3/NIH [91]. Once harvested at the appropriate concentration cells were pelletized through centrifugation (125g for 7min) and media solution was aspirated off. Cell pellets were then suspended in 1mL of the 2% alginate solution mixed by a 1000µL micropipette to ensure even distribution of the cells within the construct. The 1mL of alginate mixture containing cells was then cast in a 24-well culture plate. The dispensed gel was then crosslinked with 500µL of 2% CaCl2 for 5 minutes before being immersed in wells of 1mL of 2% CaCl2 to improve the strength and structural integrity of the cross-linked hydrogel. This resulted in Ø12x10mm thick cast constructs containing 5million cells encased in alginate hydrogel. The constructs were then each stored in a well of a 6 well plate containing 4mL of media at 37°C

(5% CO2) for 24 hours to mitigate the risk of the external stimuli from the casting process interfering with the dielectric readings of each cellular construct [92].

4.4. Drug Dispensing

For cellular constructs that underwent drug screening a drug solution containing acetaminophen was prepared. Acetaminophen (APAP, Sigma-Aldrich) was UV sterilized prior to being mixed with prepared media at the following concentrations: 0.25g/mL, 0.5g/mL, 1g/mL so that when submerged in 4mL of media the constructs would be exposed to the following concentrations of acetaminophen: 1g, 2g, 4g along with a control of 0g that consisted of media without the addition of acetaminophen. Constructs that were used in drug screening trials were then placed into a 6 well plate with 4mL of media containing acetaminophen for 24 hours for cells to metabolize the drug.

4.5. Assays

LIVE/DEAD® assay (Life Technologies, Carlsbad, CA) was prepared by mixing 5µL calcein and 20µL ethidine into 10mL of PBS before applying 1mL doses on cellular constructs followed by an hour of incubation. Subsequently, the discs were imaged using a fluorescence microscope (DM5500B, Leica Microsystems, Wetzlar, Germany) to qualify the cellular viability.

alamarBlue (aB) assay (Thermo Fisher Scientific) was used to quantify the metabolic rate of cellular constructs. aB was dispensed at 400µL doses onto cellular constructs housed in 3.6mL media within a 6 well plate. After 5 hours three 1 ml samples from each well were transferred to a 24 well plate placed on a micro-plate reader (Tecan, Männedorf, Switzerland), and analyzed for absorbance at 570 nm and 600 nm excitation and emission wavelengths, respectively. The absorbance data was reported as % aB reduction after normalizing to the acellular control.

alamarBlue assay curve was prepared using three distinct cell concentrations of 1 million, 2 million and 5 million cells. Trend lines were generated to quantify cell population given a alamarBlue reduction rate.

4.6. Dielectric Spectroscopy Assessment Methodology

The dielectric permittivity spectra, of each construct, was measured using a dielectric spectroscopy flush probe (Ø25mm; ABER Instruments Ltd., Aberystwyth, UK) with a set up as shown in Figure 6. On days of measurement samples of the cellular constructs were initially submerged in 1mL of $CaCl_2$ to improve the strength and structural integrity of the cross-linked hydrogel that had degraded during the time incubating in media. After being rinsed via submerging in 1mL phosphate buffer saline to prevent any ions from affecting the dielectric readings the dielectric probe was prepared for measuring the dielectric properties of each sample.

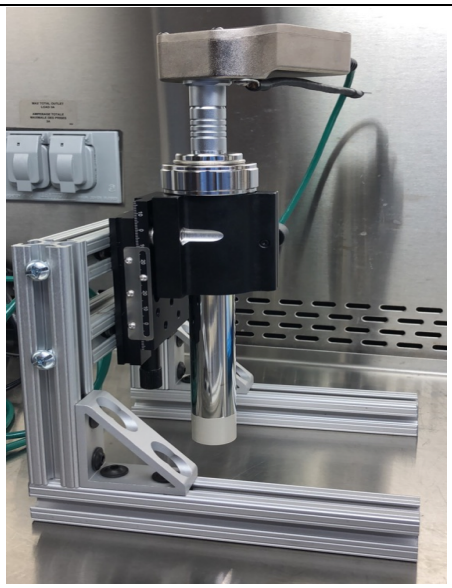

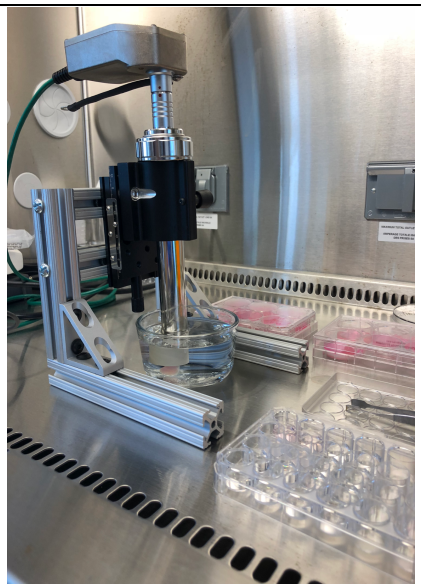

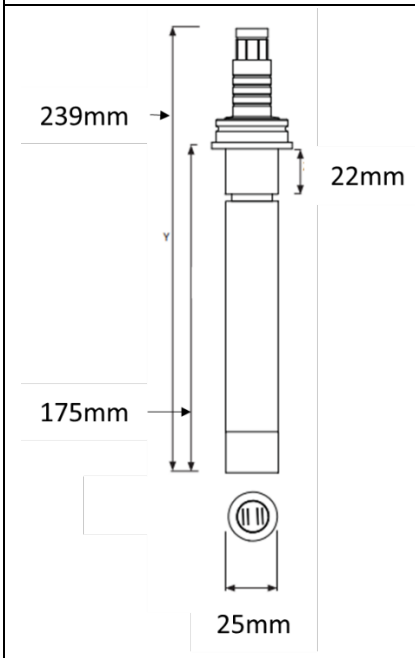

Frequency Range:50 kHz-20,000 kHz
Measuring Range:
Capacitance- 0.0 to 400 pF/cm
Conductivity- 1.0 to 40 mS/cm
Cell Concentration Range:
Yeast (6 µm Ø)- 10^6 to 10^{10} cells/mL
Bacteria (1 µm Ø)- 10^9 to 10^{13} cells/mL
Animal Cell (12 µm Ø)- 10^5 to 10^9 cells/mL
Plant Cell (50 µm Ø)- 10^3 to 10^7 cells/mL
Resolution: 0.1 pF/cm
Accuracy: ±3% of reading
Stability: ±0.2 pF/
Linearity: ±1% over 100pF/cm
Precision: ±5pF/cm

Figure 6: Set up of ABER FUTURA probe and specifications

During each experiment, the cellular construct was placed directly underneath the probe electrodes inside a glass beaker (Pyrex, Corning, NY) containing 150mL of phosphate buffer saline. Prior to the introduction of samples in each experiment, the electrodes of the probe

were cleaned using a pulse function that prevents any electrode polarization from impacting readings [93]. The total capacitance of the beaker content was measured and zeroed prior to introducing the construct. The measured capacitance was normalized using the probe constant to obtain the permittivity of the constructs.

Once placed into the experimental set up, test samples were exposed to the electric field established by the two sets of platinum electrodes on the bottom of the probe. Exposure lasted 20min in which changes in electric field due to the capacitance of cells were amplified, processed and recorded as permittivity readings across the default frequency scan (50–20,000kHz) using FUTURA SCADA (ABER Instruments Ltd.).

4.7. alamarBlue Assay Curve

Each type of cellular construct was prepared using three different concentrations- 1million cells/construct, 2million cells/construct and 5million cells/construct- to generate an alamarBlue assay curve based on the reduction percentage of each concentration (n=3). Constructs were cast using the methods detailed in Section 4.3. and alamarBlue was administered using the methods detailed in Section 4.5. Once reduction rates were obtained the average of each concentration was plotted in MS Excel using a scatterplot to establish a line of best fit that details the predicted alamarBlue reduction rate corresponding to the number of cells within a cellular construct.

4.8. Data Analysis

A standard frequency scan of 50-20,000 kHz was performed on each construct, and data from the 16 preset frequencies between 50-2115 kHz (50, 64, 82, 106, 136, 174, 224, 287, 368, 473, 607, 779, 1000, 1284, 1648 and 2115 kHz), as recommended for mammalian cell culture, was used for β-dispersion characterization. β-dispersion curves of the constructs were created by plotting the relative permittivity against log scale frequency [73,94]. The

permittivity values at different frequencies are reported as an average of the permittivity readings over a 20-minute measurement interval. The $\Delta\varepsilon$, α, and f_c values were determined from these β-dispersion curves. Using MS Excel each spectra of permittivity readings were plotted in response to frequency. From these graphs, the $\Delta\varepsilon$ was calculated as the difference in relative permittivity between the low-frequency high-plateau and high-frequency low-plateau regions of the curve. The f_c was determined by fitting a sixth-degree polynomial to the decline region of the curve and solving for the frequency at a relative permittivity value of $\Delta\varepsilon/2$. The α was calculated as the slope of the decline region of the curve. The statistical software package JMP was used to assess statistical significance through ANOVA and Tukey Post Hoc tests.

CHAPTER 5: RESULTS AND DISCUSSION

5.1 Research Objective 1

For DS to be an effective tool of PAT, it must be able to track changes over time and have reliable feedback that indicates changes in biofabricated constructs. To assess this, Research Objective 1 investigates the responses in dielectric parameters when cellular constructs are maintained over an extended period of time. In accordance to the design of experiments layout of the QbD framework, CQA must be quantified and have an established relationship to Q-TPP. To establish this, assays were cross-referenced with dielectric responses to quantify the CQA of viable cell population.

Permittivity readings of cellular alginate constructs (n = 3) were monitored over the course of 5 days at 48 hour intervals of time lapse. Each sample's permittivity readings were then analyzed through MS Excel to determine the dielectric properties of each sample. Next, the dielectric properties of each sample were analyzed for significance using the statistical software JMP.

Table 1: Experimental design for Research Objective 1

Factors	**Levels**	**Samples**
Cell Type	NIH/3T3, HepG2, Co-Culture	n = 3
Day	Day 1, Day 3, Day 5	
Responses	$\Delta\varepsilon$, α, aB% and f_c	

Two-way ANOVA results show that the day that monitoring took place had a significant effect on $\Delta\varepsilon$ ($p < 0.0001$) with a corresponding significant effect on the percentage of alamarBlue reduction (aB%) between days ($p < 0.0001$). Tukey HSD post-hoc tests show that $\Delta\varepsilon$ readings on Day 3 was statistically significant from Day 1 and Day 5 across all three

types of cellular constructs ($p < 0.05$), but differences between Day 1 and Day 5 were not significant.

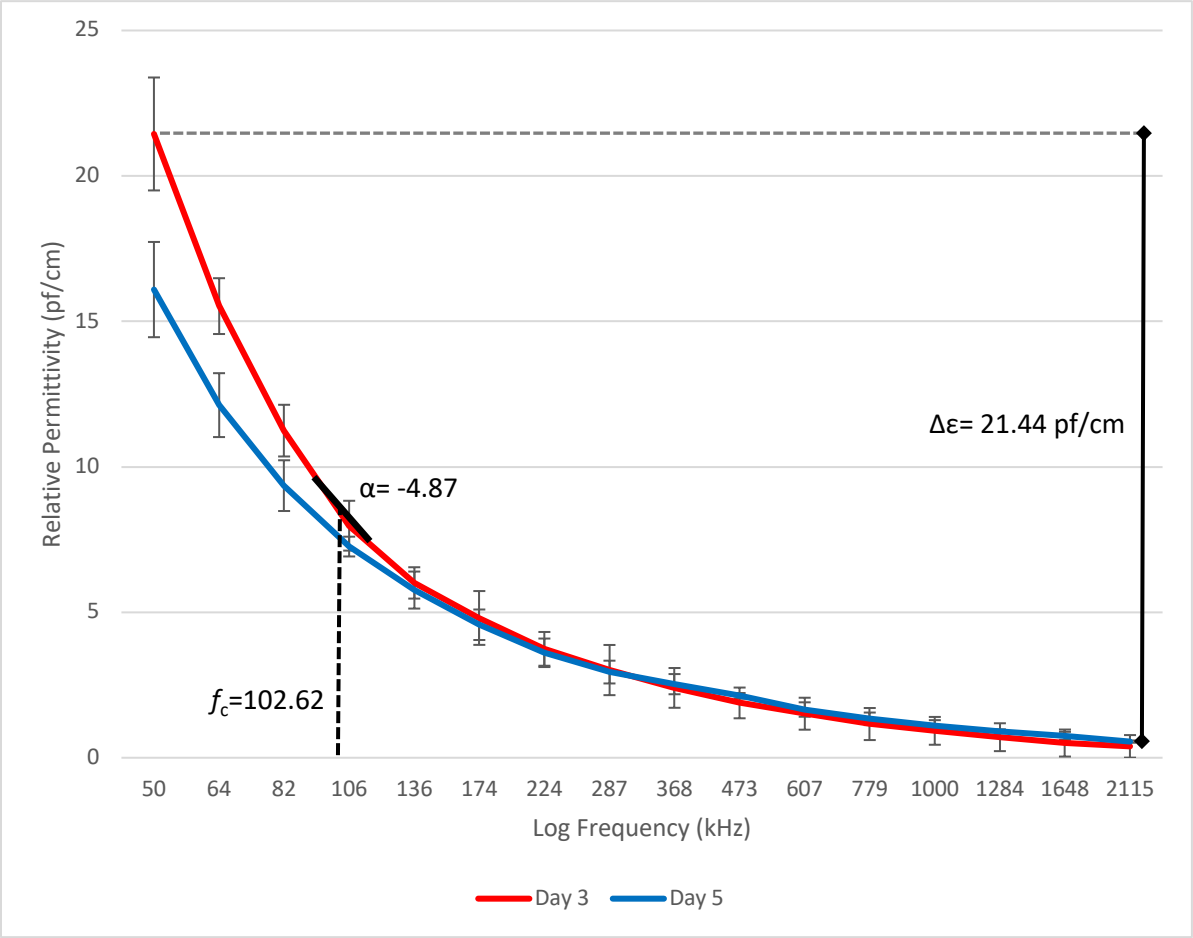

Figure 7: β-dispersion for HepG2 on Day 3 compared to Day 5 with the dielectric parameters for HepG2 on Day 3 noted

Tukey HSD post-hoc tests show that for each cellular construct type aB% coincides with the changes noted in Δε i.e. a significant difference in Day 3, while Day 1 and Day 5 are not significantly different ($p< 0.05$). This supports the concept of Δε permittivity as a measure of viable cell population and is confirmed by prior research on alginate hydrogels that note its inefficacy for long-term studies [95].

To establish the relationship between the Δε readings and the CQA of viable cell population, alamarBlue assay curves were prepared for each of the three cellular construct types. The aB% for each cell type for each given day was then quantified to estimate the viable cell population. Other methods of quantifying cell count involve dissociating the cells from encapsulation, but this can have harmful effects on cells, reducing viability in the processes [96].

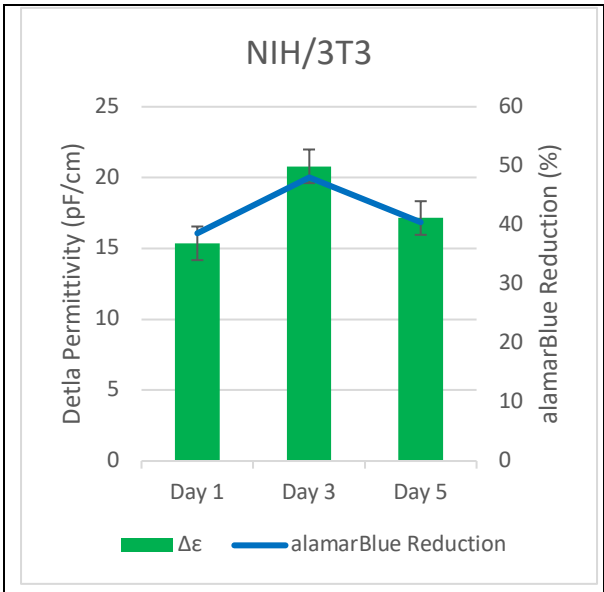

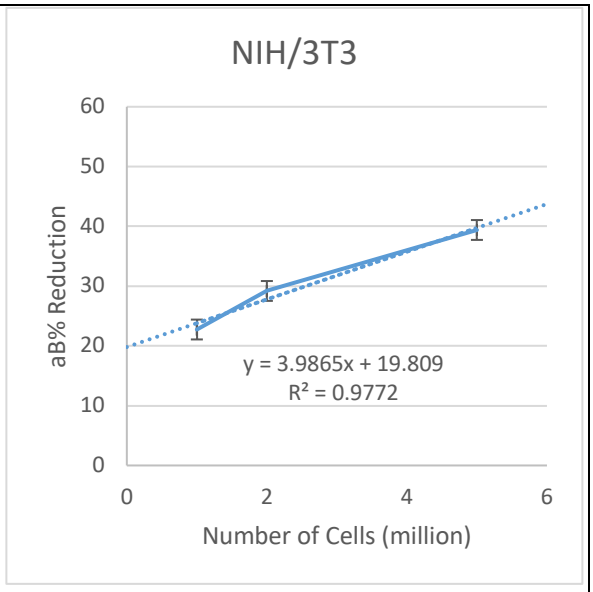

Day 1	Δε = 15.36 pF/cm	aB% = 38.57%	Cell Estimate = 4.71mil
Day 3	Δε = 20.80 pF/cm	aB% = 48.03%	Cell Estimate = 7.08mil
Day 5	Δε = 17.15 pF/cm	aB% = 40.44%	Cell Estimate = 5.18mil

Figure 8: Top Left: Δε for NIH/3T3 cellular constructs and corresponding alamarBlue Reduction % across each day of dielectric monitoring. Top Right: An alamarBlue assay curve with line of best fit based off aB% for 1 million, 2 million and 5 million cells per NIH/3T3 cellular construct. Bottom: Corresponding Δε, aB% and estimates of cell count per sample based on alamarBlue assay curve

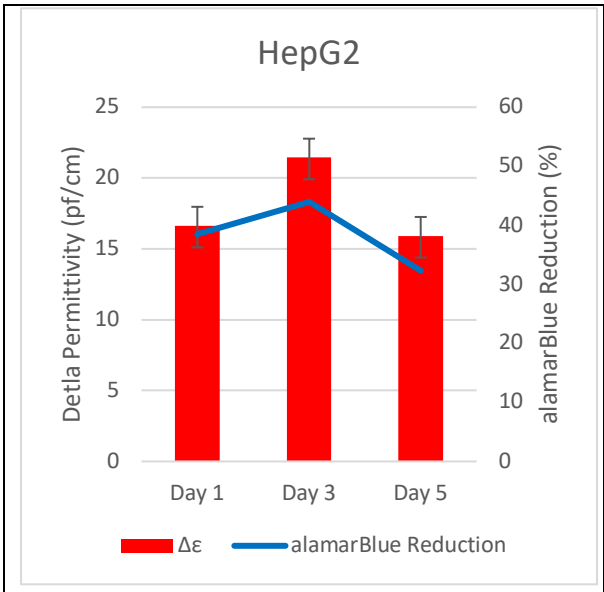

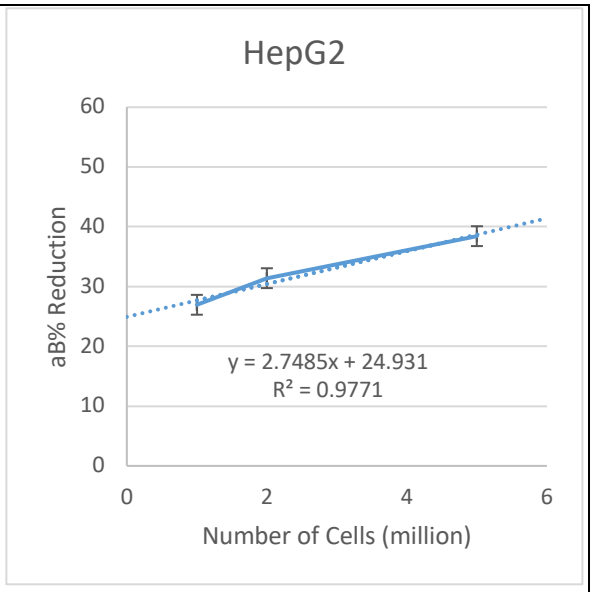

Day 1	Δε = 16.64 pF/cm	aB% = 38.52%	Cell Estimate = 4.94mil
Day 3	Δε = 21.44 pF/cm	aB% = 43.96%	Cell Estimate = 6.92mil
Day 5	Δε = 15.92 pF/cm	aB% = 32.32%	Cell Estimate = 2.69mil

Figure 9: Top Left: Δε for HepG2 cellular constructs and corresponding alamarBlue Reduction % across each day of dielectric monitoring. Top Right: An alamarBlue assay curve with line of best fit based off aB% for 1 million, 2 million and 5 million cells per HepG2 cellular construct. Bottom: Corresponding Δε, aB% and estimates of cell count per sample based on alamarBlue assay curve

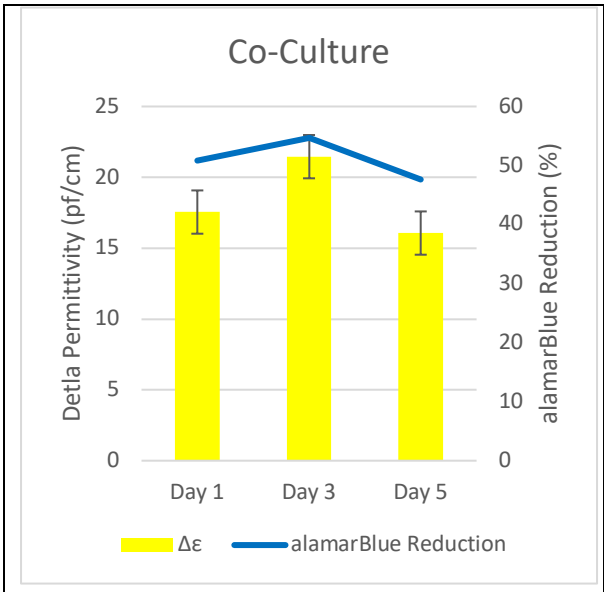

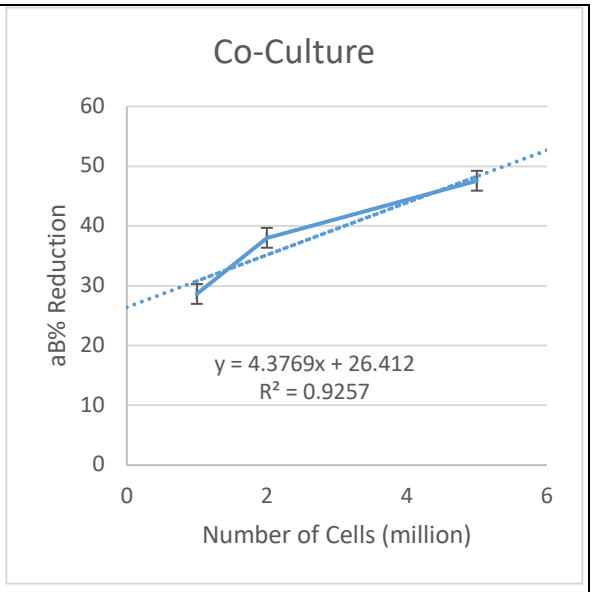

Day 1	Δε = 17.55 pF/cm	aB% = 50.79%	Cell Estimate = 5.56mil
Day 3	Δε = 21.46 pF/cm	aB% = 54.68%	Cell Estimate = 6.46mil
Day 5	Δε = 16.07 pF/cm	aB% = 47.63%	Cell Estimate = 4.84mil

Figure 10: Top Left: Δε for Co-Culture cellular constructs and corresponding alamarBlue Reduction % across each day of dielectric monitoring. Top Right: An alamarBlue assay curve with line of best fit based off aB% for 1 million, 2 million and 5 million cells per Co-Culture cellular construct. Bottom: Corresponding Δε, aB% and estimates of cell count per sample based on alamarBlue assay curve

Results from two-way ANOVA indicate that α, and f_c were not significant different across cell types, day of monitoring or any interaction between the two factors. aB% between cell type was significant ($p < 0.0001$) supporting studies that demonstrate different metabolic rates between cell types [97].

Given the similarities in cell radius, the insignificant difference between the dielectric responses of each cell type is reasonable.

Table 2: Dielectric parameters of each cell type measured for Research Objective 1 on Day 1 of the study

Cell Type	Δε (pF/cm)	f_c (kHz)	α	aB%	Ø (μm)
NIH/3T3	15.36	110.86	-3.90	38.57	18
HepG2	16.64	113.49	-5.12	38.52	18
Co-Culture	17.55	97.30	-4.19	50.79	18

5.2 Research Objective 2

Drug screening is likely the most imminent application of biofabrication. With the capability to perform on-line quality monitoring with real-time feedback, DS has the potential to assess the changes in cells overtime when exposed to drugs. This continuous monitoring would enable a better understanding of changes in cellular morphology as drugs are metabolized. To this point, studies were performed to investigate the efficacy of DS in the application of drug screening.

Cellular alginate constructs (n= 3) were administered different doses of acetaminophen- 0g (control), 1g, 2g, 4g. After a 24 hour time lapse, for cells to metabolize the drug, monitoring of the permittivity of each sample was performed with subsequent analysis to determine the dielectric properties of each sample. Samples of the same cell type and drug concentration were then analyzed through the statistical software JMP to determine significance of findings.

Table 1: Experimental design for Research Objective 2

Factors	**Levels**	**Samples**
Cell Type	NIH/3T3, HepG2, Co-Culture	n = 3
Drug Dosage	0g, 1g, 2g, 4g of Acetaminophen	
Responses	Δε, α, aB% and f_c	

Two-way ANOVA results show that Δε, α, aB% and f_c were all significantly affected by cell type, drug concentration and the interaction between both factors ($p < 0.05$). Tukey HSD post-hoc tests showed no notable difference across any administered drug dosage for cellular constructs consisting of NIH/3T3 cells for α, aB% and f_c while Δε was not significantly different between 0g, 1g and 2g, but there was significant difference between 1g and 2g when compared to 4g. When drug dosage was compared within cell type via Tukey HSD post-hoc test, both HepG2 and the Co-Culture cellular constructs showed no significant difference between 0g, 1g and 2g for Δε, α, and f_c ($p < 0.05$), but both 4g drug dosage groups had significant difference from the other drug dosage groups ($p < 0.05$). aB% significantly lowered when drugs were applied, but there were no notable differences between the three different drug doses: 1g, 2g and 4g.

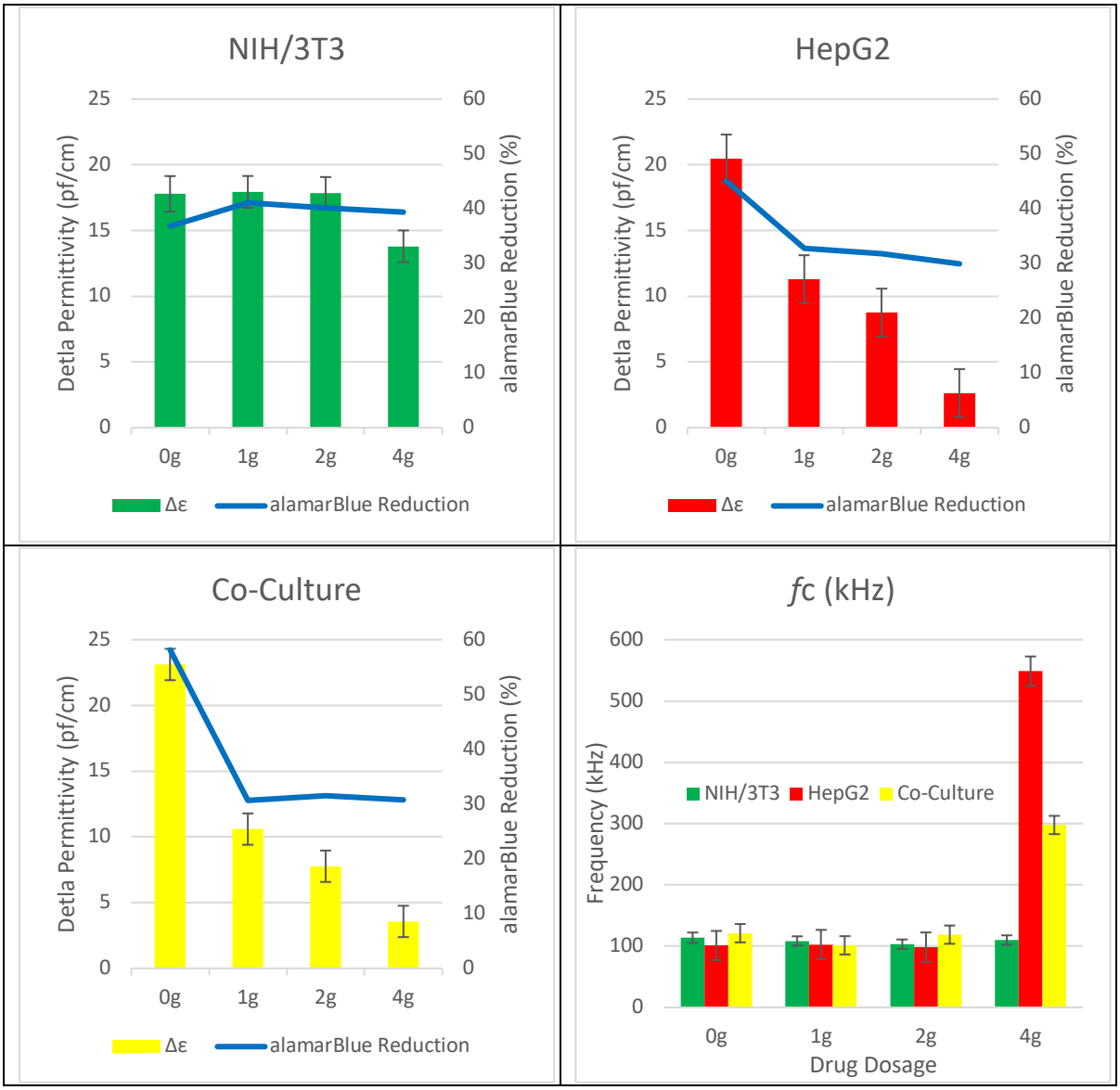

Figure 11: Comparisons of $\Delta\varepsilon$ between cell types when exposed to different doses of acetaminophen and the f_c value

The decrease in Δε of HepG2 and Co-Culture cellular constructs is supported by LIVE/DEAD that was performed on separate samples to qualify the amount of cells that were dying under drug exposure. Across all samples exposed to 0g APAP, we observe nearly 100% viability (as indicated by the green staining) with very little cell death (as indicated by

red staining) that occurred through processing to make the cellular constructs. However, when LIVE/DEAD was performed on samples that were exposed to 4g of APAP, cell death in HepG2 and Co-Culture cellular constructs exceeded cell death that occurred in NIH/3T3 samples. This is supported by drug study research that indicates hepatocytes undergo necrosis and apoptosis while fibroblasts do not undergo cytotoxic effects [98]. The accurate monitoring and real-time feedback provided by DS supports use for detecting cell death that occurs as a product of drug screening.

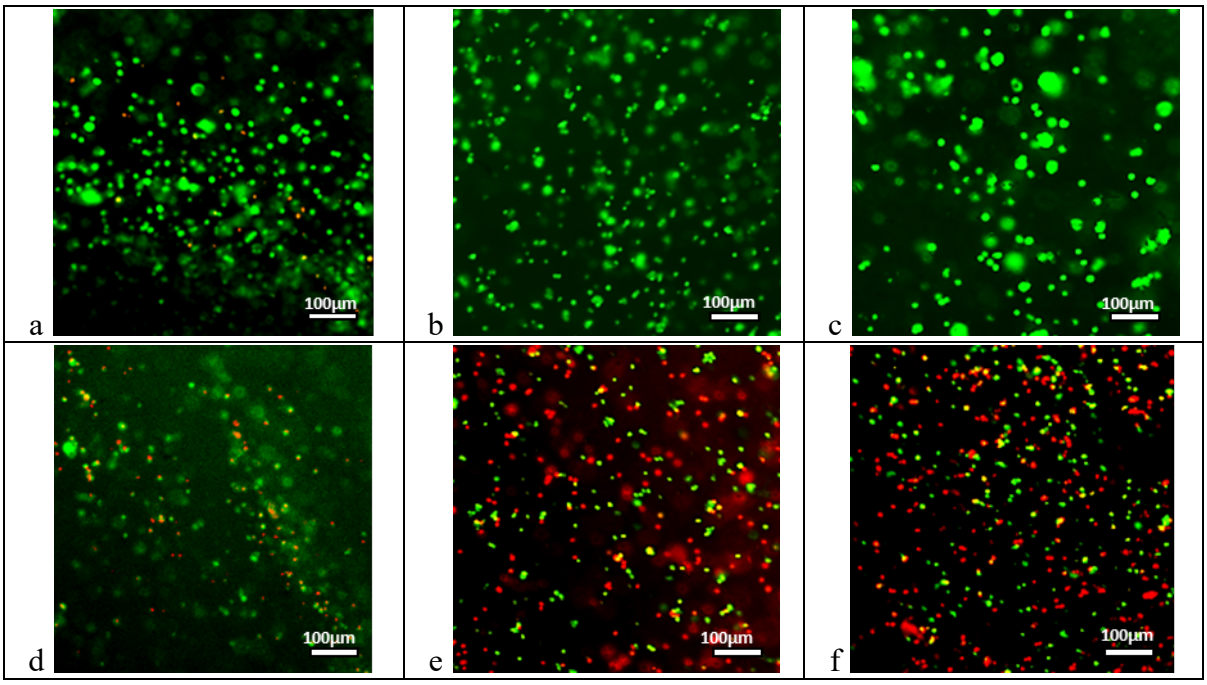

Figure 12: LIVE/DEAD images of biofabricated constructs consisting of (a) NIH/3T3 cells exposed to 0g APAP (b) HepG2 cells exposed to 0g APAP (c) Co-culture of NIH/3T3 and HepG2 cells exposed to 0g APAP (d) NIH/3T3 cells exposed to 4g APAP (e) HepG2 cells exposed to 4g APAP (f) Co-Culture of NIH/3T3 and HepG2 cells exposed to 4g APAP

When observing the permittivity readings of samples consisting of HepG2 or Co-Culture cellular constructs exposed to 4g of acetaminophen, a shift in the β-dispersion is noted. Samples that are unexposed to APAP exhibit a steep slope beginning at the first preset frequency of the ABER probe permittivity readings (50 kHz). This is observed across all

three types of cellular constructs when exposed to 0g; the same trends are present in Research Objective 1 for all three days of measurement. However, when exposed to 4g APAP both HepG2 and Co-Culture cellular constructs provide permittivity readings that signify a shift in β-dispersion. For HepG2, in particular, this shift occurs by a rising permittivity reading until reaching a permittivity value of 136 kHz before the permittivity readings decrease resulting in the steady slope that is associated with the β-dispersion.

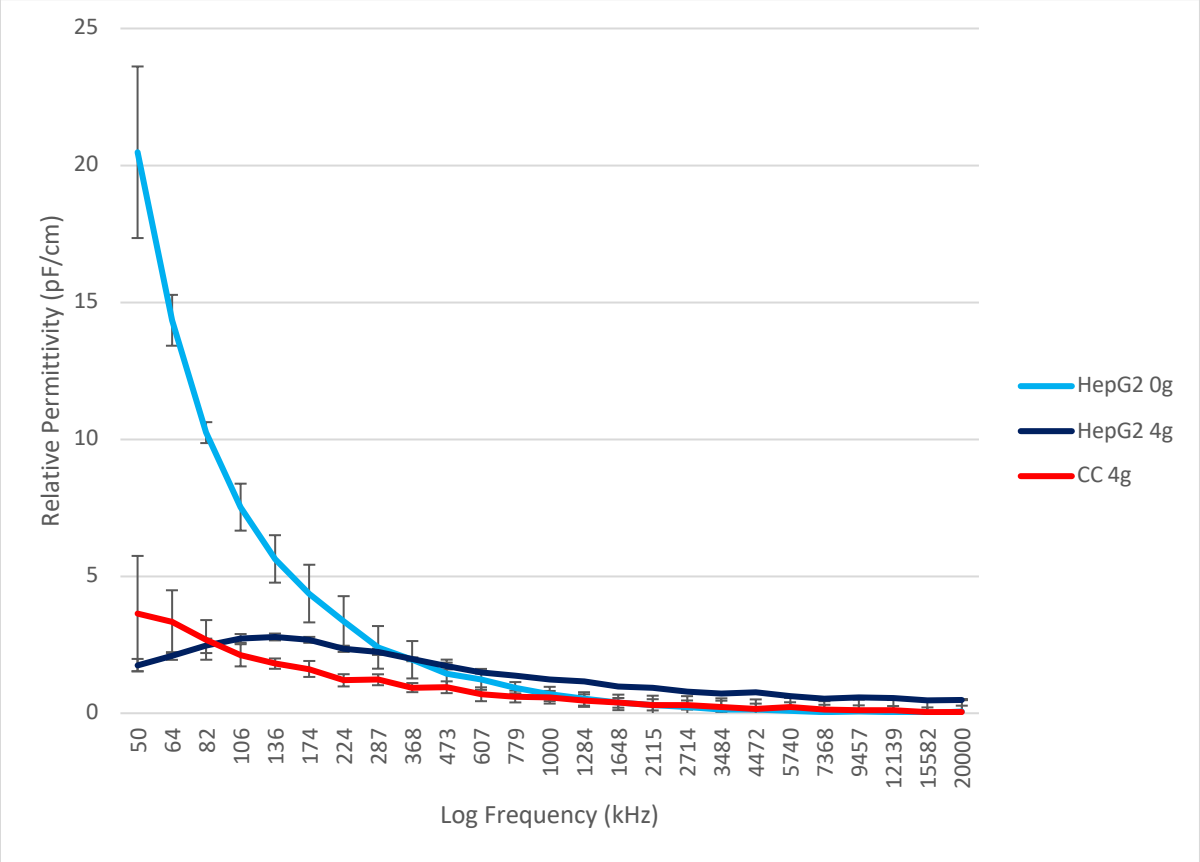

Figure 13: β-dispersion of HepG2 with 0g of APAP, HepG2 with 4g of APAP and Co-Culture with 4g of APAP

This shift in β-dispersion has the most impact on f_c, resulting in a shift to high frequencies as the β-dispersion begins at higher frequencies. Given the connection between acetaminophen induced hepatotoxicity and apoptosis, a relationship can be made to Equation 2 in which f_c

has an inverse relationship to cell radius [99–101]. Recall that hepatocytes undergo necrosis while fibroblasts do not experience it when exposed to APAP, the significant difference between each of the three types of cellular construct's f_c ($p < 0.05$) can likely be attributed to hepatotoxicity causing shrinkage of HepG2 cells that are undergoing apoptosis while dielectric readings are taken [98].

	NIH/3T3				HepG2			
Dose	Δε (pf/cm)	f_c (kHz)	α	aB%	Δε (pf/cm)	f_c (kHz)	α	aB%
0g	17.79	113.70	-4.46	36.79	20.48	101.00	-4.49	45.07
1g	17.94	108.40	-5.21	41.07	11.30	102.72	-2.39	32.71
2g	17.86	103.26	-4.70	40.10	8.75	98.49	-1.77	31.78
4g	13.80	110.00	-5.68	39.39	2.63	548.88	-1.80	29.92

	Co-Culture			
Dose	Δε (pf/cm)	f_c (kHz)	α	aB%
0g	23.12	121.17	-7.51	58.15
1g	10.60	101.38	-3.90	30.67
2g	7.77	118.80	-2.41	31.57
4g	3.57	297.71	-1.09	30.73

Figure 14: Dielectric parameters of each cell type after exposure to specified dose of Acetaminophen during the study for Research Objective 2

The detected shift in the β-dispersion and the corresponding changes to f_c complex cellular reactions to drug screening are shown to be distinguishable through monitoring of dielectric parameters. This evidence supports the use of DS as a nondestructive means of providing real-time feedback while drug screening occurs.

5.3. Chapter Summary

The Δε values for each of the three cell types fabricated into cellular constructs- NIH/3T3, HepG2, co-culture of NIH/3T3 and HepG2- changed significantly over the course of 5 days

when measured every 48hours. This change, corresponding with alamarBlue reduction rates, indicates that the cell population increased from Day 1 to Day 3 before the population decreased on Day 5. This is supported by other studies conducted using sodium alginate, which has not shown the ability to withstand cell life for long term studies. Through correspondence with alamarBlue assay curve the cell population of each sample where quantified, further supporting the findings. While the $\Delta\varepsilon$ values significantly changed, all other dielectric properties did not change between days. Given that f_c and α are properties inherent to cell type and cell distribution, respectively, the lack of change corresponds to dielectric theory and the insignificant variation is promising for the use of DS to track dielectric changes over time.

When acetaminophen was applied for 24hours the dielectric parameters of both the HepG2 and co-culture cellular constructs changed significantly. Changes were most notable when comparing the control of 0g APAP applied to 4g APAP applied in which $\Delta\varepsilon$ dropped significantly as cell death occurred (as supported the LIVE/DEAD assay). Additionally, when comparing permittivity readings of HepG2 or Co-Culture constructs exposed to 4g of APAP a shift in the β-dispersion resulting in a higher f_c value leading to the conclusion that the cells undergo apoptosis resulting in shrinkage.

CHAPTER 6: CONCLUSIONS

6.1. Conclusions and Contributions

This thesis investigates the efficacy of using dielectric spectroscopy as a means of PAT for biofabrication to enable QbD upon industry scale-up and to provide real-time feedback of biofabricated constructs. Impetus to do so sources from the knowledge gap of current cell quality assessment requiring destructive sampling, lag time for processing or inaccuracies due to design optimization for 2D systems, not 3D. Contributions to the field of biofabrication include the support for DS as a method of PAT within the QbD framework; this enables scale-up of biofabrication from research settings to industry level production. This investigation quantifies dielectric properties to estimated cell counts through the use of assays, establishing the connection between DS, CQA and Q-TPP. Drug screening studies demonstrated the ability to monitor changes in cellular constructs via DS, a significant contribution that updates previous methods that involved destructive sampling or lag time that were unable track responses to drugs over long term studies.

6.2. Future Work

6.2.1. Inclusion of DS for On-Line Monitoring of Bioprints

The QbD framework promotes the use of on-line quality monitoring to facilitate an integrated and robust approach to quality. The use dielectric spectroscopy as PAT for the QbD system has been strongly supported through the results of both research objectives. Although the real-time feedback of DS was shown, an integrated, on-line monitoring method was not a part of any of the studies in this paper. To test the potential DS shows for quality monitoring in the field of biofabrication future work should integrate DS into the process flow of manufacturing biofabricated constructs to assess the utility of on-line assessments.

6.2.2. Dielectric Probe Studies

To expand on the work done on this paper the method of measurement will need to be more thoroughly optimized. Studies should be conducted using a more sensitive dielectric probe that could be used to assess the permittivity spectra of cells at a lower frequency (<50kHz) to gather more data about the α-dispersion and to ensure that the β-dispersion is beginning at the slope that is captured starting at 50kHz using the ABER FUTURA probe. Additionally, although this study indicates low variability in terms of repeatability (results between experimental runs), reproducibility (results between operators) should be analyzed to ensure results do not change significantly if a different operator takes readings using the same set up. This would be achieved through a Gage R&R study

6.2.3. More Complex Cellular Constructs for Drug Modeling

While co-culture cellular constructs are more indicative of organ function than single cell constructs multi-cellular constructs that incorporate more cell lines would better indicate drug toxicity. Further studies should be designed to include more cell lines that are found in the liver, most notably endothelial cells to provide a cellular system with normal, abnormal and tumor-associated angiogenesis, oxidative stress, hypoxia and inflammation related pathways in endothelia under normal and pathological conditions that better models toxicity [102,103].

6.2.4. Imaging Cellular Constructs

To better understand the changes in cellular morphology that occur in response to drug exposure further imaging could take place. Ideally this imaging would enable quantification of membrane thickness and cell radius after drugs have been metabolized. As previously mentioned, confirmation of cell viability and morphology by dissociation of alginate is problematic, but if a different material or method was used to separate the cells from

encapsulation then further analysis and imaging could better confirm theories of cell shrinkage and cell death.

As biofabrication continues to grow and DS is considered as a quality monitoring technique further research will be needed to confirm the efficacy of DS as a method of real-time, on-line feedback that is needed for PAT. These future directions would give a more robust application of DS to the field of biofabrication resulting in a better system for quality assessment.

REFERENCES

[1] Viola, J., Lal, B., and Grad, O., 1987, "The Emergence of Tissue Engineering as a Research Field," New Dir. Youth Dev., **2010**(126), pp. 7–12.

[2] Brown, P. T., Handorf, A. M., Jeon, W. B., and Li, W.-J., 2013, "Stem Cell-Based Tissue Engineering Approaches for Musculoskeletal Regeneration.," Curr. Pharm. Des., **19**(19), pp. 3429–45.

[3] Wu, L. Q., and Payne, G. F., 2004, "Biofabrication: Using Biological Materials and Biocatalysts to Construct Nanostructured Assemblies," Trends Biotechnol., **22**(11), pp. 593–599.

[4] Groll, J., Boland, T., Blunk, T., Burdick, J. A., Cho, D.-W., Dalton, P. D., Derby, B., Forgacs, G., Li, Q., Mironov, V. A., Moroni, L., Nakamura, M., Shu, W., Takeuchi, S., Vozzi, G., Woodfield, T. B. F., Xu, T., Yoo, J. J., and Malda, J., 2016, "Biofabrication: Reappraising the Definition of an Evolving Field.," Biofabrication, **8**(1), p. 013001.

[5] Malda, J., Visser, J., Melchels, F. P., Jüngst, T., Hennink, W. E., Dhert, W. J. A., Groll, J., and Hutmacher, D. W., 2013, "25th Anniversary Article: Engineering Hydrogels for Biofabrication," Adv. Mater., **25**(36), pp. 5011–5028.

[6] Hait, W. N., 2010, "Anticancer Drug Development: The Grand Challenges," Nat. Rev. Drug Discov., **9**(4), pp. 253–254.

[7] NELITA T. ELLIOTT, F. Y. D., 2011, "A Review of Three-Dimensional In Vitro Tissue Models for Drug Discovery and Transport Studies," J. Pharm. Sci., **100**, pp. 59–74.

[8] Lieschke, G. J., and Currie, P. D., 2007, "Animal Models of Human Disease: Zebrafish Swim into View," Nat. Rev. Genet., **8**(5), pp. 353–367.

[9] Dongeun Huh, Benjamin D. Matthews, Akiko Mammoto, Martín Montoya-Zavala, Hong Yuan Hsin, D. E. I., 2010, "Reconstituting Organ-Level Lung," Science (80-.)., **328**(June), pp. 1662–1669.

[10] Melchels, F. P. W., Feijen, J., and Grijpma, D. W., 2010, "A Review on Stereolithography and Its Applications in Biomedical Engineering," Biomaterials, **31**(24), pp. 6121–6130.

[11] Wang, Z., Abdulla, R., Parker, B., Samanipour, R., Ghosh, S., and Kim, K., 2015, "A Simple and High-Resolution Stereolithography-Based 3D Bioprinting System Using Visible Light Crosslinkable Bioinks," Biofabrication, **7**(4).

[12] Melchels, F. P. W., Domingos, M. A. N., Klein, T. J., Malda, J., Bartolo, P. J., and Hutmacher, D. W., 2012, "Additive Manufacturing of Tissues and Organs," Prog. Polym. Sci., **37**(8), pp. 1079–1104.

[13] Pati, F., Jang, J., Ha, D. H., Won Kim, S., Rhie, J. W., Shim, J. H., Kim, D. H., and Cho, D. W., 2014, "Printing Three-Dimensional Tissue Analogues with Decellularized Extracellular Matrix Bioink," Nat. Commun., **5**, pp. 1–11.

[14] Pigott, J. H., Ishihara, A., Wellman, M. L., Russell, D. S., and Bertone, A. L., 2013, "Investigation of the Immune Response to Autologous, Allogeneic, and Xenogeneic Mesenchymal Stem Cells after Intra-Articular Injection in Horses," Vet. Immunol. Immunopathol., **156**(1–2), pp. 99–106.

[15] Gerlach, C., Johnen, C., Mccoy, E., Bra, K., and Corcos, A., 2011, "Autologous Skin Cell Spray-Transplantation for a Deep Dermal Burn Patient in an Ambulant Treatment Room Setting," **37**, pp. 19–23.

[16] Zuk, P. A., Zhu, M., Mizuno, H., Huang, J. I., Futrell, W. J., Katz, A. J., Benhaim, P., Lorenz, H. P., and Hedrick, M. H., 2001, "Multilineage Cells from Human Adipose Tissue: Implications for Cell-Based Therapies.," Tissue Eng., **7**(2), pp. 211–28.
[17] Ozbolat, I. T., 2015, "Bioprinting Scale-up Tissue and Organ Constructs for Transplantation," Trends Biotechnol., **33**(7), pp. 395–400.
[18] Melchels, F. P. W., Domingos, M. A. N., Klein, T. J., Malda, J., Bartolo, P. J., and Hutmacher, D. W., 2012, "Additive Manufacturing of Tissues and Organs," Prog. Polym. Sci., **37**(8), pp. 1079–1104.
[19] Löffelholz, C., Husemann, U., Greller, G., Meusel, W., Kauling, J., Ay, P., Kraume, M., Eibl, R., and Eibl, D., 2013, "Bioengineering Parameters for Single-Use Bioreactors : Overview and Evaluation of Suitable Methods," (1), pp. 40–56.
[20] Ingber, D. E., 2002, "Mechanical Signaling and the Cellular Response to Extracellular Matrix in Angiogenesis and Cardiovascular Physiology," Circ. Res., **91**(10), pp. 877–887.
[21] Brandl, F., Sommer, F., and Goepferich, A., 2007, "Rational Design of Hydrogels for Tissue Engineering: Impact of Physical Factors on Cell Behavior," Biomaterials, **28**(2), pp. 134–146.
[22] Wyllie, A. H., 1997, "Apoptosis : An Overview," **53**(3), pp. 451–465.
[23] Gregory, C. A., Gunn, W. G., Peister, A., and Prockop, D. J., 2004, "An Alizarin Red-Based Assay of Mineralization by Adherent Cells in Culture: Comparison with Cetylpyridinium Chloride Extraction," Anal. Biochem., **329**(1), pp. 77–84.
[24] Rampersad, S. N., 2012, "Multiple Applications of Alamar Blue as an Indicator of Metabolic Function and Cellular Health in Cell Viability Bioassays," pp. 12347–12360.
[25] Riss, T. L., Niles, A. L., and Minor, L., 2015, "Cell Viability Assays," Assay Guid. Man. [Internet], pp. 1–23.
[26] Monteiro-Riviere, N. A., Inman, A. O., and Zhang, L. W., 2009, "Limitations and Relative Utility of Screening Assays to Assess Engineered Nanoparticle Toxicity in a Human Cell Line," Toxicol. Appl. Pharmacol., **234**(2), pp. 222–235.
[27] P., B., A., S., K., S., R., S., A., W., J., J., and P., G., 2006, "Introduction to in Vitro Estimation of Metabolic Stability and Drug Interactions of New Chemical Entities in Drug Discovery and Development," Pharmacol. Reports, **58**(4), pp. 453–472.
[28] Sin, A., Chin, K. C., Jamil, M. F., Kostov, Y., Rao, G., and Shuler, M. L., 2004, "The Design and Fabrication of Three-Chamber Microscale Cell Culture Analog Devices with Integrated Dissolved Oxygen Sensors," Biotechnol. Prog., **20**(1), pp. 338–345.
[29] Fey, S. J., and Wrzesinski, K., 2012, "Determination of Drug Toxicity Using 3D Spheroids Constructed from an Immortal Human Hepatocyte Cell Line," Toxicol. Sci., **127**(2), pp. 403–411.
[30] Zhang, L., and Mao, S., 2017, "Application of Quality by Design in the Current Drug Development," Asian J. Pharm. Sci., **12**(1), pp. 1–8.
[31] Yu, L. X., 2013, "Quality by Design (QbD): A New Concept for Development of Quality Pharmaceuticals," Int. J. Pharm. Qual. Assur., **4**(2), pp. 13–19.
[32] Huang, J., Kaul, G., Cai, C., Chatlapalli, R., Hernandez-Abad, P., Ghosh, K., and Nagi, A., 2009, "Quality by Design Case Study: An Integrated Multivariate Approach to Drug Product and Process Development," Int. J. Pharm., **382**(1–2), pp. 23–32.
[33] Rathore, A. S., 2009, "Roadmap for Implementation of Quality by Design (QbD) for

Biotechnology Products," Trends Biotechnol., **27**(9), pp. 546–553.
[34] Conference, I., Harmonisation, O. N., Technical, O. F., For, R., Of, R., For, P., and Use, H., 2009, "International Conference on Harmonisation (ICH) of Technical Requirement for Registration of Pharmaceuticals for Human Use, Pharmaceutical Development, Q8 (R2), ICH, August 2009," **8**(August).
[35] Goetze, A. M., Schenauer, M. R., and Flynn, G. C., 2010, "Assessing Monoclonal Antibody Product Quality Attribute Criticality through Clinical Studies," MAbs, **2**(5), pp. 500–507.
[36] Horvath, B., Mun, M., and Laird, M. W., 2010, "Characterization of a Monoclonal Antibody Cell Culture Production Process Using a Quality by Design Approach," Mol. Biotechnol., **45**(3), pp. 203–206.
[37] Zupke, C., Brady, L. J., Slade, P. G., Clark, P., Caspary, R. G., Livingston, B., Taylor, L., Bigham, K., Morris, A. E., and Bailey, R. W., 2015, "Real-Time Product Attribute Control to Manufacture Antibodies with Defined N-Linked Glycan Levels," Biotechnol. Prog., **31**(5), pp. 1433–1441.
[38] FDA, 2004, "Guidance for Industry PAT: A Framework for Innovative Pharmaceutical Development, Manufacuring, and Quality Assurance," FDA Off. Doc., (September), p. 16.
[39] Foley, W. J., McIlwee, A., Lawler, I., Aragones, L., Woolnough, A. P., and Berding, N., 1998, "Ecological Applications of near Infrared Reflectance Spectroscopy - A Tool for Rapid, Cost-Effective Prediction of the Composition of Plant and Animal Tissues and Aspects of Animal Performance," Oecologia, **116**(3), pp. 293–305.
[40] DiMasi, J. A., Hansen, R. W., and Grabowski, H. G., 2003, "The Price of Innovation: New Estimates of Drug Development Costs," J. Health Econ., **22**(2), pp. 151–185.
[41] Vogt, F. G., and Kord, A. S., 2011, "Development of Quality-by-Design Analytical Methods," J. Pharm. Sci., **100**(3), pp. 797–812.
[42] Bordawekar, S., Chanda, A., Daly, A. M., Garrett, A. W., Higgins, J. P., LaPack, M. A., Maloney, T. D., Morgado, J., Mukherjee, S., Orr, J. D., Reid, G. L., Yang, B. S., and Ward, H. W., 2015, "Industry Perspectives on Process Analytical Technology: Tools and Applications in API Manufacturing," Org. Process Res. Dev., **19**(9), pp. 1174–1185.
[43] Rüdt, M., Briskot, T., and Hubbuch, J., 2017, "Advances in Downstream Processing of Biologics – Spectroscopy: An Emerging Process Analytical Technology," J. Chromatogr. A, **1490**, pp. 2–9.
[44] Kourti, T., 2006, "Process Analytical Technology beyond Real-Time Analyzers: The Role of Multivariate Analysis," Crit. Rev. Anal. Chem., **36**(3–4), pp. 257–278.
[45] Pittenger, M. F., Mackay, A. M., Beck, S. C., Jaiswal, R. K., Mosca, J. D., Moorman, M. A., Simonetti, D. W., Craig, S., Marshak, D. R., Pittenger, M. F., Mackay, A. M., Beck, S. C., Jaiswal, R. K., Douglas, R., Mosca, J. D., Moorman, M. A., Simonetti, D. W., Craig, S., and Marshak, D. R., 2016, "Multilineage Potential of Adult Human Mesenchymal Stem Cells," Am. Assoc. Adv. Sci. Stable, **284**(5411), pp. 143–147.
[46] Murphy, S. V., and Atala, A., 2014, "3D Bioprinting of Tissues and Organs," Nat. Biotechnol., **32**(8), pp. 773–785.
[47] Zhang, A. P., Qu, X., Soman, P., Hribar, K. C., Lee, J. W., Chen, S., and He, S., 2012, "Rapid Fabrication of Complex 3D Extracellular Microenvironments by Dynamic Optical Projection Stereolithography," Adv. Mater., **24**(31), pp. 4266–4270.

[48] Choi, Y. J., Yi, H. G., Kim, S. W., and Cho, D. W., 2017, "3D Cell Printed Tissue Analogues: A New Platform for Theranostics," Theranostics, **7**(12), pp. 3118–3137.
[49] Olson, J. L., Atala, A., and Yoo, J. J., 2011, "Tissue Engineering: Current Strategies and Future Directions," Chonnam Med. J., **47**(1), p. 1.
[50] Bauwens, C. L., Peerani, R., Niebruegge, S., Woodhouse, K. A., Kumacheva, E., Husain, M., and Zandstra, P. W., 2008, "Control of Human Embryonic Stem Cell Colony and Aggregate Size Heterogeneity Influences Differentiation Trajectories," Stem Cells, **26**(9), pp. 2300–2310.
[51] Miller, J. S., 2014, "The Billion Cell Construct: Will Three-Dimensional Printing Get Us There?," PLoS Biol., **12**(6), pp. 1–9.
[52] Dalton, A. C., and Barton, W. A., 2014, "Over-Expression of Secreted Proteins from Mammalian Cell Lines," Protein Sci., **23**(5), pp. 517–525.
[53] Gregory, C. D., Pound, J. D., Devitt, A., Wilson-Jones, M., Ray, P., and Murray, R. J., 2010, "Inhibitory Effects of Persistent Apoptotic Cells on Monoclonal Antibody Production in Vitro," MAbs, **1**(4), pp. 370–376.
[54] Browne, S. M., and Al-Rubeai, M., 2011, "Defining Viability in Mammalian Cell Cultures," Biotechnol. Lett., **33**(9), pp. 1745–1749.
[55] Morgan, H., Sun, T., Holmes, D., Gawad, S., and Green, N. G., 2007, "Single Cell Dielectric Spectroscopy," J. Phys. D Appl. Phys, **40**, pp. 61–70.
[56] Folgero, K., Friiso, T., Hilland, J., and Tjomsland, T., 1995, "A Broad-Band and High-Sensitivity Dielectric-Spectroscopy Measurement System for Quality Determination of Low-Permittivity Fluids," Meas. Sci. Technol., **6**(7), pp. 995–1008.
[57] Cole, K. S., and Cole, R. H., 1941, "Dispersion and Absorption in Dielectrics I. Alternating Current Characteristics," J. Chem. Phys., **9**(4), pp. 341–351.
[58] O'Neill, D., Bowman, R. M., and Gregg, J. M., 2000, "Dielectric Enhancement and Maxwell–Wagner Effects in Ferroelectric Superlattice Structures," Appl. Phys. Lett., **77**(10), p. 1520.
[59] O'Neill, D., Bowman, R. M., and Gregg, J. M., 2000, "Dielectric Enhancement and Maxwell-Wagner Effects in Ferroelectric Superlattice Structures," Appl. Phys. Lett., **77**(10), pp. 1520–1522.
[60] Liu, J., Duan, C. G., Mei, W. N., Smith, R. W., and Hardy, J. R., 2005, "Dielectric Properties and Maxwell-Wagner Relaxation of Compounds ACu 3Ti 4O 12 (A=Ca,Bi 2/3 ,Y 2/3,La 2/3)," J. Appl. Phys., **98**(9), pp. 1–6.
[61] Lunkenheimer, P., Bobnar, V., Bobnar, V., Pronin, A. V., Pronin, A. V., Ritus, A. I., Volkov, A. A., and Loidl, A., 2002, "Origin of Apparent Colossal Dielectric Constants," Phys. Rev. B - Condens. Matter Mater. Phys., **66**(5), pp. 521051–521054.
[62] Matthews, G. G., 2013, "App.3 Electrical Properties of Cells," Cell. Physiol. Nerve Muscle.
[63] Shi, J., Aisaki, K., Ikawa, Y., and Wake, K., 1998, "Evidence of Hepatocyte Apoptosis in Rat Liver after the Administration of Carbon Tetrachloride," Am. J. Pathol., **153**(2), pp. 515–525.
[64] Gujral, J. S., Knight, T. R., Farhood, A., Bajt, M. L., and Jaeschke, H., 2002, "Mode of Cell Death after Acetaminophen Overdose in Mice: Apoptosis or Oncotic Necrosis?," Toxicol. Sci., **67**(2), pp. 322–328.
[65] Jack A. Hinson, Dean W. Roberts, and L. P. J., 2010, *Mechanisms of Acetaminophen-Induced Liver Necrosis Jack*.

[66] Cannizzaro, C., Gügerli, R., Marison, I., and Von Stockar, U., 2003, "On-Line Biomass Monitoring of CHO Perfusion Culture With Scanning Dielectric Spectroscopy," Biotechnol. Bioeng., **84**(5), pp. 597–610.
[67] Gheorghiu, E., 1996, "Measuring Living Cells Using Dielectric Spectroscopy," **40**, pp. 0–6.
[68] Heileman, K., Daoud, J., and Tabrizian, M., 2013, "Dielectric Spectroscopy as a Viable Biosensing Tool for Cell and Tissue Characterization and Analysis," Biosens. Bioelectron., **49**, pp. 348–359.
[69] Asami, K., and Yonezawa, T., 1996, "Dielectric Behavior of Wild-Type Yeast and Vacuole-Deficient Mutant over a Frequency Range of 10 KHz to 10 GHz," Biophys. J., **71**(4), pp. 2192–2200.
[70] Davey, C. L., Davey, H. M., Kell, D. B., and Todd, R. W., 1993, "Introduction to the Dielectric Estimation of Cellular Biomass in Real Time, with Special Emphasis on Measurements at High Volume Fractions," Anal. Chim. Acta, **279**(1), pp. 155–161.
[71] McRae, D. a, and Esrick, M. a, 1996, "Deconvolved Electrical Impedance Spectra Track Distinct Cell Morphology Changes.," IEEE Trans. Biomed. Eng., **43**(6), pp. 607–18.
[72] Zhang, M. I. N., Repo, T., Willison, J. H. M., and Sutinen, S., 1995, "Electrical Impedance Analysis in Plant Tissues: On the Biological Meaning of Cole-Cole Alpha in Scots Pine Needles," Eur. Biophys. J., **24**(2), pp. 99–106.
[73] Siano, S. A., 1997, "Biomass Measurement by Inductive Permittivity," Biotechnol. Bioeng., **55**(2), pp. 289–304.
[74] Ansorge, S., Esteban, G., and Schmid, G., 2007, "On-Line Monitoring of Infected Sf-9 Insect Cell Cultures by Scanning Permittivity Measurements and Comparison with off-Line Biovolume Measurements," Cytotechnology, **55**(2–3), pp. 115–124.
[75] Ansorge, S., Esteban, G., and Schmid, G., 2010, "Multifrequency Permittivity Measurements Enable On-Line Monitoring of Changes in Intracellular Conductivity Due to Nutrient Limitations during Batch Cultivations of CHO Cells," Biotechnol. Prog., **26**(1), pp. 272–283.
[76] Khamzin, A. A., Nigmatullin, R. R., and Popov∗, I. I., 2012, "Microscopic Model of a Non-Debye Dielectric Relaxation : The Cole – Cole Law and Its Generalization," Theor. Math. Phys., **173**(2), pp. 1604–1619.
[77] Cao, W., and Gerhardt, R., 1990, "Calculation of Various Relaxation Times and Conductivity for a Single Dielectric Relaxation Process," Solid State Ionics, **42**(3–4), pp. 213–221.
[78] Markx, G. H., and Davey, C. L., 1999, "The Dielectric Properties of Biological Cells at Radiofrequencies: Applications in Biotechnology," Enzyme Microb. Technol., **25**(3–5), pp. 161–171.
[79] Daoud, J., Asami, K., Rosenberg, L., and Tabrizian, M., 2012, "Dielectric Spectroscopy for Non-Invasive Monitoring of Epithelial Cell Differentiation within Three-Dimensional Scaffolds," Phys. Med. Biol., **57**(16), pp. 5097–5112.
[80] Asami, K., 2002, "Characterization of Biological Cells by Dielectric Spectroscopy," **305**, pp. 268–277.
[81] Patel, P., and Markx, G. H., 2008, "Dielectric Measurement of Cell Death," Enzyme Microb. Technol., **43**(7), pp. 463–470.
[82] Maskow, T., Röllich, A., Fetzer, I., Ackermann, J. U., and Harms, H., 2008, "On-Line

Monitoring of Lipid Storage in Yeasts Using Impedance Spectroscopy," J. Biotechnol., **135**(1), pp. 64–70.
[83] Salonen, K. K. K., Meskanen, U. M. E., and Eerikäinen, M. L. T., 2007, "On-Line Biomass Measurements in Bioreactor Cultivations : Comparison Study of Two on-Line Probes," pp. 561–566.
[84] Laufer, S., Ivorra, A., Reuter, V. E., Rubinsky, B., and Solomon, S. B., 2010, "Electrical Impedance Characterization of Normal and Cancerous Human Hepatic Tissue," Physiol. Meas., **31**(7), pp. 995–1009.
[85] Roggo, Y., Chalus, P., Maurer, L., Lema-Martinez, C., Edmond, A., and Jent, N., 2007, "A Review of near Infrared Spectroscopy and Chemometrics in Pharmaceutical Technologies," J. Pharm. Biomed. Anal., **44**(3 SPEC. ISS.), pp. 683–700.
[86] Card, C., Hunsaker, B., Smith, T., and Hirsch, J., 2008, "Near-Infrared Spectroscopy for Rapid, Simultaneous Monitoring," Bioprocess. Int., **6**(3), pp. 58–67.
[87] Abu-Absi, N. R., Kenty, B. M., Cuellar, M. E., Borys, M. C., Sakhamuri, S., Strachan, D. J., Hausladen, M. C., and Li, Z. J., 2011, "Real Time Monitoring of Multiple Parameters in Mammalian Cell Culture Bioreactors Using an In-Line Raman Spectroscopy Probe," Biotechnol. Bioeng., **108**(5), pp. 1215–1221.
[88] Lamping, S. R., Zhang, H., Allen, B., and Ayazi Shamlou, P., 2003, "Design of a Prototype Miniature Bioreactor for High Throughput Automated Bioprocessing," Chem. Eng. Sci., **58**(3–6), pp. 747–758.
[89] Narayanan, L. K., Huebner, P., Fisher, M. B., Spang, J. T., Starly, B., and Shirwaiker, R. A., 2016, "3D-Bioprinting of Polylactic Acid (PLA) Nanofiber-Alginate Hydrogel Bioink Containing Human Adipose-Derived Stem Cells," ACS Biomater. Sci. Eng., **2**(10), pp. 1732–1742.
[90] Narayanan, L. K., Thompson, T. L., Bhat, A., Starly, B., and Shirwaiker, R. A., 2017, "Investigating Dielectric Impedance Spectroscopy As a Non-Destructive Quality Assessment Tool for 3D Cellular Constructs," ASME. Int. Manuf. Sci. Eng. Conf., **4**(Bio and Sustainable Manufacturing), p. V004T05A013.
[91] Bhatia, S. N., Yarmush, M. L., and Toner, M., 1997, "Controlling Cell Interactions by Micropatterning in Co- Cultures: Hepatocytes and 3T3 Fibroblasts," J. Biomed. Mater. Res., **34**, p. 189–199 ST–Controlling cell interactions by mic.
[92] Yang, J., Huang, Y., Wang, X., Wang, X. B., Becker, F. F., and Gascoyne, P. R., 1999, "Dielectric Properties of Human Leukocyte Subpopulations Determined by Electrorotation as a Cell Separation Criterion.," Biophys. J., **76**(6), pp. 3307–3314.
[93] Ishai, P. Ben, Talary, M. S., Caduff, A., Levy, E., and Feldman, Y., 2013, "Electrode Polarization in Dielectric Measurements: A Review," Meas. Sci. Technol., **24**(10).
[94] Justice, C., Brix, A., Freimark, D., Kraume, M., Pfromm, P., Eichenmueller, B., and Czermak, P., 2011, "Process Control in Cell Culture Technology Using Dielectric Spectroscopy," Biotechnol. Adv., **29**(4), pp. 391–401.
[95] Lan, S. F., Safiejko-Mroczka, B., and Starly, B., 2010, "Long-Term Cultivation of HepG2 Liver Cells Encapsulated in Alginate Hydrogels: A Study of Cell Viability, Morphology and Drug Metabolism," Toxicol. Vitr., **24**(4), pp. 1314–1323.
[96] Kuen Yong Lee, and David J. Mooney, 2000, "Alginate: Properties and Biomedical Applications," Prog. Polym. Sci., **37**(1), pp. 106–126.
[97] Jimenez, A. G., Van Brocklyn, J., Wortman, M., and Williams, J. B., 2014, "Cellular Metabolic Rate Is Influenced by Life-History Traits in Tropical and Temperate Birds,"

PLoS One, **9**(1).
[98] Yu, Y. L., Yiang, G. T., Chou, P. L., Tseng, H. H., Wu, T. K., Hung, Y. T., Lin, P. S., Lin, S. Y., Liu, H. C., Chang, W. J., and Wei, C. W., 2014, "Dual Role of Acetaminophen in Promoting Hepatoma Cell Apoptosis and Kidney Fibroblast Proliferation," Mol. Med. Rep., **9**(6), pp. 2077–2084.
[99] Wang, K., 2014, "Molecular Mechanisms of Hepatic Apoptosis," Cell Death Dis., **5**(1), pp. e996-10.
[100] Jaeschke, H., Duan, L., Akakpo, J. Y., Farhood, A., and Ramachandran, A., 2018, "The Role of Apoptosis in Acetaminophen Hepatotoxicity," Food Chem. Toxicol., **118**(March), pp. 709–718.
[101] Piratvisuth, T., and Marcellin, P., 2011, "Further Analysis Is Required to Identify an Early Stopping Rule for Peginterferon Therapy That Is Valid for All Hepatitis B e Antigen-Positive Patients," Hepatology, **53**(3), pp. 1054–1055.
[102] Domansky, K., Inman, W., Serdy, J., Dash, A., Lim, M. H. M., and Griffith, L. G., 2010, "Perfused Multiwell Plate for 3D Liver Tissue Engineering," Lab Chip, **10**(1), pp. 51–58.
[103] Miki, Y., Ono, K., Hata, S., Suzuki, T., Kumamoto, H., and Sasano, H., 2012, "The Advantages of Co-Culture over Mono Cell Culture in Simulating in Vivo Environment," J. Steroid Biochem. Mol. Biol., **131**(3–5), pp. 68–75.

APPENDICES

Appendix A: Output of HepG2 (0g of APAP) Permittivity Readings

Frequency (kHz)	HepG2 0g		
	Sample 1	Sample 2	Sample 3
50	18.65453	24.098	18.69121
64	13.44288	15.298	14.2985
82	9.813529	10.38431	10.53843
106	7.136235	6.929	8.506786
136	5.745706	4.717308	6.438857
174	4.243	3.385923	5.479
224	3.603	2.351538	4.129571
287	2.741471	1.515462	2.958929
368	2.348765	1.164538	2.3455
473	1.832471	0.870462	1.642429
607	1.597235	0.836231	1.277571
779	1.151706	0.741077	0.899071
1000	0.994353	0.626385	0.488857
1284	0.759647	0.537615	0.2695
1648	0.622588	0.486154	0.077714
2115	0.538118	0.444538	-0.1075
2714	0.408706	0.504	-0.21764
3484	0.284882	0.443385	-0.34029
4472	0.268235	0.414308	-0.30136
5740	0.286941	0.428846	-0.44671
7368	0.194765	0.339	-0.4185
9457	0.224059	0.397	-0.41214
12139	0.207353	0.377462	-0.4545
15582	0.177529	0.311154	-0.4715
20000	0.249294	0.390769	-0.46829

Appendix B: alamarBlue Assay Curve Readings

Cell Type	Sample #	1 Million Cells	2 Million Cells	5 Million Cells
NIH/3T3	Sample 1	24.51105	28.93707	38.85367
	Sample 2	20.59213	27.07284	40.23383
	Sample 3	23.1228	31.56023	39.08711
HepG2	Sample 1	27.13397	30.31222	38.94782
	Sample 2	25.79573	32.15657	35.66677
	Sample 3	27.91564	31.73663	40.67513
Co-Culture	Sample 1	27.21	41.07	45.57
	Sample 2	29.58	35.98	47.88

	Sample 3	29.16	37.05	49.30

Appendix C: NIH/3T3 Dielectric Responses for Research Objective 1

	Day 1			Day 3		
	Sample 1	**Sample 2**	**Sample 3**	**Sample 1**	**Sample 2**	**Sample 3**
Delta C	17.60	14.24	14.25	20.17	21.46	20.76
Fc	100.01	109.70	122.78	107.48	100.41	119.73
Alpha	-3.42	-4.28	-3.99	-2.95	-3.79	-2.94
% Reduction	38.23	38.17	39.3	46.9	49.8	47.4

	Day 5		
	Sample 1	**Sample 2**	**Sample 3**
Delta C	15.49	18.29	17.68
Fc	119.03	116.81	122.89
Alpha	-3.22	-4.66	-4.92
% Reduction	38.63	41.59	41.1

Appendix D: HepG2 Dielectric Responses for Research Objective 1

	Day 1			Day 3		
	Sample 1	**Sample 2**	**Sample 3**	**Sample 1**	**Sample 2**	**Sample 3**
Delta C	17.56	16.86	15.49	20.42	24.26	19.64
Fc	105.03	110.78	124.67	98.99	104.08	124.10
Alpha	-4.35	-5.47	-5.54	-2.76	-6.70	-4.44
% Reduction	38.60	39.59	37.35	43.09	46.87	41.90

	Day 5		
	Sample 1	**Sample 2**	**Sample 3**
Delta C	14.56	15.21	17.99
Fc	104.59	95.58	116.23
Alpha	-3.32	-3.78	-3.96
% Reduction	33.43	33.02	30.52

Appendix E: Co-Culture Dielectric Responses for Research Objective 1

	Day 1			Day 3		
	Sample 1	**Sample 2**	**Sample 3**	**Sample 1**	**Sample 2**	**Sample 3**
Delta C	17.48	16.94	17.32	20.78	19.32	24.27
Fc	99.58	97.52	94.80	107.86	92.25	107.74
Alpha	-3.06	-4.24	-5.26	-4.42	-4.89	-5.30
% Reduction	50.38	51.10	50.88	54.49	55.69	53.85

	Day 5		
	Sample 1	**Sample 2**	**Sample 3**
Delta C	17.46	15.19	15.55
Fc	109.68	103.64	116.96
Alpha	-4.47	-4.35	-3.76
% Reduction	45.50	49.79	47.60

Appendix F: NIH/3T3 Dielectric Responses for Research Objective 2

		Delta C	Fc	Alpha	% Reduction
	Sample 1	17.05	114.87	-3.90	38.85
3T3 Control	**Sample 2**	18.53	112.53	-5.01	34.72
	Sample 1	17.61	106.00	-4.61	42.48
	Sample 2	19.25	95.94	-3.70	39.67
3T3 1g	**Sample 3**	16.96	123.26	-7.33	-
	Sample 1	15.43	110.46	-4.34	38.79
	Sample 2	19.30	99.17	-4.73	41.41
3T3 2g	**Sample 3**	18.84	100.16	-5.64	-
	Sample 1	14.92	101.42	-5.11	38.34
	Sample 2	13.82	109.51	-4.82	40.44
3T3 4g	**Sample 3**	12.65	119.07	-7.12	-

Appendix G: HepG2 Dielectric Responses for Research Objective 2

		Delta C	Fc	Alpha	% Reduction
	Sample 1	18.48	105.26	-4.53	49.06
	Sample 2	23.79	89.63	-2.98	40.38
HepG2 Control	**Sample 3**	19.16	108.11	-5.97	45.76
	Sample 1	10.86	110.50	-2.44	35.01
	Sample 2	9.21	106.55	-2.35	34.16
HepG2 1g	**Sample 3**	13.81	91.11	-2.37	28.96
	Sample 1	11.11	109.12	-2.21	31.93
	Sample 2	8.97	87.08	-1.86	35.03
HepG2 2g	**Sample 3**	6.18	99.28	-1.24	28.40
	Sample 1	2.64	530.05	-1.60	30.94
	Sample 2	2.37	505.13	-1.90	32.26
HepG2 4g	**Sample 3**	2.89	611.46	-1.90	26.56

Appendix H: Co-Culture Dielectric Responses for Research Objective 2

		Delta C	Fc	Alpha	% Reduction
	Sample 1	25.48	132.99	-9.06	64.91
	Sample 2	22.30	112.21	-6.69	55.37
CC Control	**Sample 3**	21.57	118.31	-6.77	54.15
	Sample 1	11.61	96.08	-2.55	31.96
	Sample 2	9.41	96.05	-1.99	33.30
CC 1g	**Sample 3**	10.78	112.00	-7.16	26.75
	Sample 1	8.67	113.77	-2.19	36.19
	Sample 2	7.23	112.10	-2.94	32.15
CC 2g	**Sample 3**	7.20	130.54	-2.11	26.36
	Sample 1	2.44	276.65	-1.02	34.25
	Sample 2	2.98	281.65	-1.05	31.96
CC 4g	**Sample 3**	5.29	334.82	-1.20	25.98